

Generalized Intersection Algorithms with Fixpoints for Image Decomposition Learning

Robin Richter*, Duy H. Thai[†] and Stephan F. Huckemann*

October 20, 2020

Abstract

In image processing, classical methods minimize a suitable functional that balances between computational feasibility (convexity of the functional is ideal) and suitable penalties reflecting the desired image decomposition. The fact that algorithms derived from such minimization problems can be used to construct (deep) learning architectures has spurred the development of algorithms that can be trained for a specifically desired image decomposition, e.g. into cartoon and texture. While many such methods are very successful, theoretical guarantees are only scarcely available. To this end, in this contribution, we formalize a general class of intersection point problems encompassing a wide range of (learned) image decomposition models, and we give an existence result for a large subclass of such problems, i.e. giving the existence of a fixpoint of the corresponding algorithm. This class generalizes classical model-based variational problems, such as the TV- ℓ^2 -model or the more general TV-Hilbert model. To illustrate the potential for learned algorithms, novel (non learned) choices within our class show comparable results in denoising and texture removal.

1 Introduction

Decomposing an image into parts that carry desired information and other parts that are considered as nuisance is an old, and yet, an ever new problem. For decades this problem has been attacked under a variational paradigm crafting suitable objective functions that reflect a desired image decomposition, e.g. [SGG⁺09, CCN15]. Often, however, it is not fully clear, how optimal these objective functions are for a given task. Typically for cartoon-texture decomposition, there are three goals: identifying piecewise constant parts, keeping contrast and avoiding artefacts. For this and other tasks such as denoising/deblurring or classification, see e.g. [KBPS11, BP10, SB07, MMG12, BBD⁺06, YGO05].

Exploiting recently developed (convolutional) neural networks, improved objective functions have been *learned*, e.g. [MJU17, Wan16]. Also, since solutions of minimization problems are often obtained algorithmically, and every iteration step can be viewed as applying a family of convolution filters, suitable filters have

*R. Richter and S.F. Huckemann are with the Felix-Bernstein-Institute for Mathematical Statistics in the Biosciences at the University of Goettingen, 37077 Goettingen, Germany (e-mails: robin.richter@mathematik.uni-goettingen.de, huckeman@math.uni-goettingen.de)

[†]D.H. Thai is with the Department of Mathematics at Colorado State University

been learned (e.g. [CYP15, CP17, AÖ17, AÖ18, YSLX16, LCG18]). Corresponding solutions are often no longer minimizers of an (explicitly given) objective function, e.g. [YSLX16, LCG18]. While, corresponding algorithms come naturally with an explicit *intersection problem* – the solution of which are fixed points – as the connection with an objective function may be lost, it is a priori unclear whether fixed points exist at all.

In our contribution we prove that fixed points exist for a large class of intersection problems. This class encompasses many classical models such as the TV- ℓ^2 -model or the more general TV-Hilbert model, but is much larger. For a family of (convolution) filters that is not learned – applying our result to learned and learning filters is the subject of ongoing research – we illustrate that keeping contrast and avoiding artefacts can be achieved by convolution filters that do not correspond, to the best of the authors’ knowledge, to a minimization problem.

Throughout this contribution we consider

- an $n \times m$ pixel image given by a gray value matrix $F \in \mathbb{R}^{n \times m}$,
- a filter matrix $A \in \mathbb{R}^{n \times m}$ and families of matrix filters $\underline{B}, \tilde{\underline{B}} \in (\mathbb{R}^{n \times m})^{\times P}$ of fixed length $P \in \mathbb{N}$ inducing *discrete convolutional operators* \mathfrak{C}_A and $\underline{\mathfrak{C}}_{\underline{B}}, \underline{\mathfrak{C}}_{\tilde{\underline{B}}}$, respectively, with adjoints \mathfrak{C}_A^* , etc., as detailed in Convention 2.1.
- *shrinkage functions* S_κ ($\kappa = 1, 2$) and norms $|\cdot|_{1, \kappa}$ for $(\mathbb{R}^{n \times m})^{\times P}$, also detailed in Convention 2.1.,
- the desired output matrix $U \in \mathbb{R}^{n \times m}$, which in the context of this contribution is a denoised image (cf. Section 5.1) or a *cartoon* (cf. Section 5.2),

and the intersection Problem 1.1 below. In this and Algorithm 1.2 further below the superscript “ G ” stands for the generalization from the literature (e.g. [WT10]) and the subscript “ C ” for the constraining condition and step, respectively (see (3.1 in Section 3)).

Problem 1.1. Find $(U^\dagger, \underline{W}^\dagger, \underline{\lambda}^\dagger) \in \Omega_1^\kappa \cap \Omega_2^G \cap \Omega_C \subset (\mathbb{R}^{n \times m})^{\times (1+2P)}$ where

$$\begin{aligned} \Omega_1^\kappa &:= \left\{ (U, \underline{W}, \underline{\lambda}) \in (\mathbb{R}^{n \times m})^{\times (1+2P)} : \underline{W} = S_\kappa \left(\underline{\mathfrak{C}}_{\underline{B}}(U) - \frac{1}{\beta} \underline{\lambda}; \frac{1}{\beta} \right) \right\}, \\ \Omega_2^G &:= \left\{ (U, \underline{W}, \underline{\lambda}) \in (\mathbb{R}^{n \times m})^{\times (1+2P)} : U = \mathfrak{C}_A(F) + \underline{\mathfrak{C}}_{\tilde{\underline{B}}}^* \left(\underline{W} + \frac{1}{\beta} \underline{\lambda} \right) \right\}, \\ \Omega_C &:= \left\{ (U, \underline{W}, \underline{\lambda}) \in (\mathbb{R}^{n \times m})^{\times (1+2P)} : \underline{\mathfrak{C}}_{\underline{B}}(U) = \underline{W} \right\}. \end{aligned} \quad (1.1)$$

In order to solve Problem 1.1, we formalize a generalization of an *augmented Lagrangian/alternating method of multipliers* (AL/ADMM) algorithm originally introduced for problems of the form (1.3) below, by [EB92, Gab83], which, in our general setting rewrites as follows.

Algorithm 1.2. For $\tau = 1, 2, \dots$, do until $\frac{\|U^{(\tau)} - U^{(\tau-1)}\|}{\|U^{(\tau-1)}\|} < \epsilon$

$$\begin{aligned} \underline{W}^{(\tau)} &= \mathfrak{S}_\kappa \left(\underline{\mathfrak{C}}_{\underline{B}} \left(U^{(\tau-1)} \right) - \frac{1}{\beta} \underline{\lambda}^{(\tau)}; \frac{1}{\beta} \right), \\ U^{(\tau)} &= \mathfrak{C}_A(F) + \underline{\mathfrak{C}}_{\underline{B}}^* \left(\underline{W}^{(\tau)} + \frac{1}{\beta} \underline{\lambda}^{(\tau)} \right), \\ \underline{\lambda}^{(\tau+1)} &= \underline{\lambda}^{(\tau)} + \beta \left(\underline{W}^{(\tau)} - \underline{\mathfrak{C}}_{\underline{B}}(U^{(\tau)}) \right). \end{aligned} \quad (1.2)$$

We have at once the following equivalence.

Remark 1.3. *Every intersection point of Problem 1.1 is a fixed point of Algorithm 1.2 and vice versa.*

For the class of $(A, \underline{B}, \tilde{\underline{B}}) \in (\mathbb{R}^{n \times m})^{\times(1+2P)}$ with $(\underline{B}, \tilde{\underline{B}})$ *weakly factoring* – this new concept is defined in Definition 2.2 – and satisfying a contraction and positive semi-definite condition we give in Theorem 2.5 guarantees for existence of solutions of Problem 1.1.

As insinuated above, Problem 1.1 is motivated by its applicability to a range of algorithms learning \underline{B} and $\tilde{\underline{B}}$, in particular it covers the ADMM-NET of [YSLX16, LCG18]. In order to assess the success of such algorithms in applications ([MJU17] survey such considerations) we identify special cases of Problem 1.1.

A number of learning problems ([CYP15, CP17, AÖ17, AÖ18, YSLX16, LCG18]) build on minimizing special cases of the classical ℓ^1 -regularized functional

$$\mathcal{J}_{\text{VAR}}(U) = \left| \underline{\mathfrak{C}}_{\underline{B}}(U) \right|_{1,\kappa} + \frac{\mu}{2} \|U - F\|^2 \quad (1.3)$$

(cf. [SGG⁺09]) with $\mu > 0$. This is a special case of Problem 1.1, as we will see in Section 3.1. Notably, plugging in the two-dimensional discrete gradient ∇ - which, considering periodic boundary conditions, can be written as a convolution operator - for $\underline{\mathfrak{C}}_{\underline{B}}$ ($P = 2$) and $\kappa = 2$ in (1.3) gives the classic TV- ℓ^2 minimization problem

$$\mathcal{J}_{\text{TV-}\ell^2}(U) = |\nabla U|_{1,2} + \frac{\mu}{2} \|U - F\|^2, \quad (1.4)$$

with its continuous version proposed by [ROF92].

Closely related is the *anisotropic diffusion process*, cf. [SWB⁺04]. For general choices of \underline{B} and $\tilde{\underline{B}}$, however, it seems that Problem 1.1 cannot be written as a minimization problem such as (1.3).

Aujol and Gilboa [AG06] have introduced the *TV-Hilbert* problem by applying a convolutional operator \mathfrak{C}_M to the argument of the ℓ^2 norm in (1.4). As another contribution, in Theorem 3.4, we show that for suitably chosen A and $\tilde{\underline{B}}$, the *generalized Hilbert problem*, minimizing

$$\mathcal{J}_{\text{HIL}}(U) = \left| \underline{\mathfrak{C}}_{\underline{B}}(U) \right|_{1,\kappa} + \frac{\mu}{2} \|\mathfrak{C}_M(U - F)\|^2, \quad (1.5)$$

with suitable $M \in \mathbb{R}^{n \times m}$, where its circular Fourier transform satisfies in particular $\widehat{M} \in \mathbb{R}_+^{n \times m}$, is another special case of Problem 1.1. In this context we note the introduction of the *G-norm* by Meyer [Mey01] to model texture

components. Since the G -norm is hard to compute, it has been approximated by suitably choosing \underline{B} and M in (1.5), cf. [VO03, VO04, OSV03, GLMV07].

Our paper is structured as follows. In Section 2 we introduce the discrete notation and state the existence theorem guaranteeing solutions of Problem 1.1 for $(A, \underline{B}, \underline{\tilde{B}}) \in (\mathbb{R}^{n \times m})^{\times 1+2P}$ satisfying rather broad conditions. Its proof is deferred to Section 4 with some details further deferred to the appendix. In Section 3 we link the generalized Problem 1.1 to existing minimization problems. In fact, our Algorithm 1.2 is motivated by the AL/ADMM algorithm (Algorithm 3.1, cf. [WT10, BV04]) which solves the saddle point problem (3.3), which is equivalent to (1.3). Moreover the TV -Hilbert model of [AG06] is reverse-engineered under a condition on $(A, \underline{B}, \underline{\tilde{B}}) \in (\mathbb{R}^{n \times m})^{\times 1+2P}$ stricter than needed for the existence result. In Section 5 applications are presented in the context of denoising and the separation of cartoon and texture. We conclude the paper with an outlook to filter learning.

The results presented are taken from the Ph.D thesis of the first author [Ric19].

2 Conventions and Existence Result

Although many approaches for image decomposition are derived in the continuous domain, we consider images as matrices, what they are in applications. Similarly, operators on images are computationally discretized into (families of) matrices. Particularly handy are linear operators that can be represented via multiple circular matrix convolutions, such as the discrete gradient with periodic boundary conditions or suitably redundant, discrete (wavelet) frame operators ([Mal02]), since they are easy to implement as entry-wise multiplications in the frequency domain, making vectorization redundant.

Convention 2.1. For positive integers n, m, P , let in the following $A, G \in \mathbb{R}^{n \times m}$ be matrices and $\underline{B} = (B_1, \dots, B_P), \underline{H} = (H_1, \dots, H_P) \in (\mathbb{R}^{n \times m})^P =: \Gamma_P$ matrix-families.

- (i) Denote the entries of A by $A[k, \ell]$ for $0 \leq k \leq n-1$ and $0 \leq \ell \leq m-1$. Matrix entries are indexed in $\mathbb{Z}/n\mathbb{Z} \times \mathbb{Z}/m\mathbb{Z}$ and any matrix index exceeding the range of $\{0, 1, \dots, n-1\} \times \{0, 1, \dots, m-1\}$ takes its value modulo (n, m) , encoding periodic boundary conditions.
 A^* denotes the adjoint of A , i.e. its transposed and complex conjugate, and

$$\widehat{A} = \mathfrak{F}(A) = \left(\text{trace}(F_{rs} A^T) \right)_{r=0, s=0}^{n-1, m-1}$$

its discrete circular Fourier transform, where

$$F_{r,s}[k, \ell] = e^{-\frac{2\pi i k r}{n} - \frac{2\pi i \ell s}{m}}, \quad 0 \leq r, k \leq n-1, 0 \leq s, \ell \leq m-1.$$

- (ii) The linear operator $\mathfrak{C}_A : \mathbb{R}^{n \times m} \rightarrow \mathbb{R}^{n \times m}$ denotes the *discrete circular convolution*, or short *matrix convolution*, defined for $G \in \mathbb{R}^{n \times m}$ by

$$\mathfrak{C}_A(G) = \left(\sum_{k=0}^{n-1} \sum_{\ell=0}^{m-1} A[k-r, \ell-s] G[k, \ell] \right)_{r=0, s=0}^{n-1, m-1}.$$

With the component-wise product \odot we have the well known

$$\mathfrak{C}_A(G) = \mathfrak{F}^{-1}(\widehat{A} \odot \widehat{G})$$

where $\mathfrak{F}^{-1}(G) = \frac{1}{nm} (\text{trace}(\overline{F_{rs}} G^T))_{r=0, s=0}^{n-1, m-1}$.

Further, $\underline{\mathfrak{C}}_{\underline{B}} : \mathbb{R}^{n \times m} \rightarrow \Gamma_P$ denotes the *matrix-family convolution*, defined by

$$\underline{\mathfrak{C}}_{\underline{B}}(G) = (\mathfrak{C}_{B_1}(G), \dots, \mathfrak{C}_{B_P}(G)) ,$$

and $\underline{\underline{\mathfrak{C}}}_{\underline{B}} : \Gamma_P \rightarrow \Gamma_P$ denotes the *matrix-family convolution*, defined by

$$\underline{\underline{\mathfrak{C}}}_{\underline{B}}(\underline{H}) = (\mathfrak{C}_{B_1}(H_1), \dots, \mathfrak{C}_{B_P}(H_P))$$

Moreover, $\mathfrak{E} : \mathbb{R}^{n \times m} \rightarrow \mathbb{R}^{n \times m}$ is the identity operator.

- (iii) By $\langle \cdot, \cdot \rangle$ and $\|\cdot\|$ denote the usual Euclidean inner product and norm, respectively, for vectors, matrices and families of matrices, for instance

$$\langle A, G \rangle = \text{trace}(AG^*) \text{ and } \langle \underline{B}, \underline{H} \rangle = \sum_{p=1}^P \text{trace}(B_p H_p^*) .$$

These inner products give rise to adjoint operators

$$\mathfrak{C}_A^* : \mathbb{R}^{n \times m} \rightarrow \mathbb{R}^{n \times m}, \quad \underline{\mathfrak{C}}_{\underline{B}}^* : \Gamma_P \rightarrow \mathbb{R}^{n \times m} \text{ and } \underline{\underline{\mathfrak{C}}}_{\underline{B}}^* : \Gamma_P \rightarrow \Gamma_P .$$

Verify that $\mathfrak{C}_A^* = \mathfrak{C}_C$ with $C[k, \ell] = \overline{A[-k, -\ell]}$ and $\widehat{C}[k, \ell] = \overline{\widehat{A}[k, \ell]}$ for $0 \leq k \leq n-1$ and $0 \leq \ell \leq m-1$,

$$\underline{\underline{\mathfrak{C}}}_{\underline{B}}^*(\underline{H}) = \sum_{p=1}^P \mathfrak{C}_{B_p}^*(H_p) \text{ and } \underline{\underline{\mathfrak{C}}}_{\underline{B}}(\underline{H}) = (\mathfrak{C}_{B_1}^*(H_1), \dots, \mathfrak{C}_{B_P}^*(H_P)) .$$

- (iv) Introduce more norms by

$$\begin{aligned} \|\underline{B}\|_{1,2} &:= \sum_{k=0}^{n-1} \sum_{\ell=0}^{m-1} \|(B_1[k, \ell], \dots, B_P[k, \ell])\| , \\ \|\underline{B}\|_{1,1} &:= \sum_{p=1}^P \sum_{k=0}^{n-1} \sum_{\ell=0}^{m-1} |B_p[k, \ell]| . \end{aligned}$$

These are related to the *isotropic ℓ^1 -norm* and the *anisotropic ℓ^1 -norm*, respectively, from [CDOS12] in the continuous setting.

- (v) For $\beta \in \mathbb{R}_+$ define the *anisotropic soft-shrinkage function* $S_1 : \Gamma_P \times \mathbb{R}_+ \rightarrow \Gamma_P$ by

$$S_1(\underline{B}, \beta) := \left((s_1(B_p[k, \ell], \beta))_{k=0, \ell=0}^{n-1, m-1} \right)_{1 \leq p \leq P} ,$$

$$\text{with } s_1(x, \beta) := \begin{cases} x - \beta & \text{if } x > \beta \\ 0 & \text{if } x \in [-\beta, \beta] , \\ x + \beta & \text{if } x < -\beta \end{cases} ,$$

and the *isotropic soft-shrinkage function* $\mathsf{S}_2 : \Gamma_P \times \mathbb{R}_+ \rightarrow \Gamma_P$ by

$$\mathsf{S}_2(\underline{B}, \beta) := \left(\left(\mathsf{s}_2 \left(\left((B_p[k, \ell])_{p=1}^P \right)^T, \beta \right) [p] \right)_{k=0, \ell=0}^{n-1, m-1} \right)_{1 \leq p \leq P},$$

with

$$\mathsf{s}_2(x, \beta) := \frac{x}{\|x\|} \max(0, \|x\| - \beta)$$

for $x \in \mathbb{R}^P$.

The following definition gives a class of input filters for which Theorem 2.5 below asserts that Problem 1.1 features an intersection point and equivalently Algorithm 1.2 a fixed point (cf. Remark 1.3). It also gives a smaller class for which the minimization Problem (1.5) can be reverse engineered as an instance of Problem 1.1 in Theorem 3.4 of Section 3.2.

Definition 2.2. We call a triple $(A, \underline{B}, \tilde{\underline{B}})$ *input filters* for Algorithm 1.2 if $A \in \mathbb{R}^{n \times m}$ and $\underline{B} = (B_p)_{p=1}^P, \tilde{\underline{B}} = (\tilde{B}_p)_{p=1}^P \in \Gamma_P$. We then say that $(\underline{B}, \tilde{\underline{B}})$

- (i) *weakly factor* if there is $\underline{Y} = (Y_p)_{p=1}^P \in \Gamma_P$, called a *weak factor* of $(\underline{B}, \tilde{\underline{B}})$, such that $\hat{Y}_p \in \mathbb{R}_+^{n \times m}$ and, for all $1 \leq p \leq P$, $0 \leq k \leq n-1$ and $0 \leq \ell \leq m-1$,

$$\hat{\tilde{B}}_p[k, \ell] = \hat{Y}_p[k, \ell] \hat{B}_p[k, \ell];$$

- (ii) *strongly factor* if there is $Y \in \mathbb{R}^{n \times m}$ called a *strong factor* of $(\underline{B}, \tilde{\underline{B}})$, such that $\hat{Y} \in \mathbb{R}_+^{n \times m}$ and, for all $1 \leq p \leq P$, $0 \leq k \leq n-1$ and $0 \leq \ell \leq m-1$,

$$\hat{\tilde{B}}_p[k, \ell] = \hat{Y}[k, \ell] \hat{B}_p[k, \ell];$$

- (iii) *satisfy the non-expansive and positive semi-definite condition* (NEPC) if

$$0 \leq \sum_{p=1}^P \overline{\hat{\tilde{B}}_p[k, \ell] \hat{B}_p[k, \ell]} \leq 1, \quad \text{for all } 0 \leq k \leq n-1 \text{ and } 0 \leq \ell \leq m-1;$$

(NEPC)

- (iv) *satisfy the contraction and positive semi-definite condition* (CPC) if

$$0 \leq \sum_{p=1}^P \overline{\hat{\tilde{B}}_p[k, \ell] \hat{B}_p[k, \ell]} < 1, \quad \text{for all } 0 \leq k \leq n-1 \text{ and } 0 \leq \ell \leq m-1.$$

(CPC)

Remark 2.3. If Y is a strong factor for $(\underline{B}, \tilde{\underline{B}})$, then $\underline{\mathfrak{C}}_{\tilde{\underline{B}}} = \underline{\mathfrak{C}}_{\underline{B}} \underline{\mathfrak{C}}_Y$, yielding in conjunction with Convention 2.1, (iii),

$$\underline{\mathfrak{C}}_{\tilde{\underline{B}}}^* = \underline{\mathfrak{C}}_Y \underline{\mathfrak{C}}_{\underline{B}}^*.$$

Similarly, if \underline{Y} is a weak factor for $(\underline{B}, \tilde{\underline{B}})$, then $\underline{\mathfrak{C}}_{\tilde{\underline{B}}} = \underline{\mathfrak{C}}_{\underline{Y}} \underline{\mathfrak{C}}_{\underline{B}}$, yielding

$$\underline{\mathfrak{C}}_{\tilde{\underline{B}}}^* = \underline{\mathfrak{C}}_{\underline{B}}^* \underline{\mathfrak{C}}_{\underline{Y}}.$$

While conditions (NEPC) and (CPC) demand in particular for all k, ℓ that

$$\sum_{p=1}^P \overline{\widehat{B}_p[k, \ell]} \widehat{B}_p[k, \ell] \in \mathbb{R},$$

this is a straightforward consequence of weakly factoring filters. The following central lemma elucidates more consequences.

Lemma 2.4. *Let $(\underline{B}, \widetilde{\underline{B}}) \in \Gamma_{2P}$ be weakly factoring. Then, $\underline{\mathfrak{C}}_{\widetilde{\underline{B}}}^* \underline{\mathfrak{C}}_{\underline{B}}$ diagonalizes and the set of non-zero eigenvalues of*

$$\underline{\mathfrak{C}}_{\widetilde{\underline{B}}}^* \underline{\mathfrak{C}}_{\underline{B}} : \mathbb{R}^{n \times m} \rightarrow \mathbb{R}^{n \times m} \quad \text{and} \quad \underline{\mathfrak{C}}_{\underline{B}} \underline{\mathfrak{C}}_{\widetilde{\underline{B}}}^* : \Gamma_P \rightarrow \Gamma_P$$

coincide and is given by the following set of real, positive numbers

$$\left\{ \sum_{p=1}^P \left(\overline{\widehat{B}_p[k, \ell]} \widehat{B}_p[k, \ell] \right) : 0 \leq k \leq n-1 \text{ and } 0 \leq \ell \leq m-1 \right\} \setminus \{0\}.$$

Proof. Recall the family $F_{r,s}$ ($0 \leq r \leq n-1$, $0 \leq s \leq m-1$) of matrices from Convention 2.1 conveying the discrete Fourier transformation. In consequence of $\overline{\widehat{F}_{r,s}} = E_{r,s}$ with $E_{r,s}[k, \ell] = \delta_{rk} \delta_{s\ell}$ ($0 \leq r, k \leq n-1$, $0 \leq s, \ell \leq m-1$), we have

$$\begin{aligned} \underline{\mathfrak{C}}_{\widetilde{\underline{B}}}^* \underline{\mathfrak{C}}_{\underline{B}} (\overline{F}_{r,s}) &= \underline{\mathfrak{C}}_{\widetilde{\underline{B}}}^* (\mathfrak{C}_{B_1} (\overline{F}_{r,s}), \dots, \mathfrak{C}_{B_P} (\overline{F}_{r,s})) \\ &= \underline{\mathfrak{C}}_{\widetilde{\underline{B}}}^* \left(\frac{1}{nm} \mathfrak{F}^{-1} (\widehat{B}_1 \odot E_{r,s}), \dots, \frac{1}{nm} \mathfrak{F}^{-1} (\widehat{B}_P \odot E_{r,s}) \right) \\ &= \underline{\mathfrak{C}}_{\widetilde{\underline{B}}}^* \left(\frac{1}{nm} \mathfrak{F}^{-1} (\widehat{B}_1[r, s] E_{r,s}), \dots, \frac{1}{nm} \mathfrak{F}^{-1} (\widehat{B}_P[r, s] E_{r,s}) \right) \\ &= \frac{1}{nm} \mathfrak{F}^{-1} \left(\sum_{p=1}^P \overline{\widehat{B}_p[r, s]} (\widehat{B}_p[r, s] E_{r,s}) \right) \\ &= \left(\sum_{p=1}^P \overline{\widehat{B}_p[r, s]} \widehat{B}_p[r, s] \right) \overline{F}_{r,s}. \end{aligned}$$

Moreover, since the $\overline{F}_{r,s}$ ($0 \leq r, k \leq n-1$, $0 \leq s, \ell \leq m-1$) span $\mathbb{R}^{n \times m}$, $\underline{\mathfrak{C}}_{\widetilde{\underline{B}}}^* \underline{\mathfrak{C}}_{\underline{B}}$ diagonalizes and all of its eigenvalues are given by

$$\left\{ \sum_{p=1}^P \left(\overline{\widehat{B}_p[k, \ell]} \widehat{B}_p[k, \ell] \right) : 0 \leq k \leq n-1 \text{ and } 0 \leq \ell \leq m-1 \right\}. \quad (2.1)$$

Further, let $\underline{Y} \in \Gamma_P$ be the weak factor of $(\underline{B}, \widetilde{\underline{B}})$ such that

$$\sum_{p=1}^P \overline{\widehat{B}_p[k, \ell]} \widehat{B}_p[k, \ell] = \sum_{p=1}^P \widehat{Y}_p[k, \ell] \left\| \widehat{B}_p[k, \ell] \right\|^2 \in \mathbb{R}_+,$$

and consider an eigenvalue $\nu \neq 0$ of $\underline{\mathfrak{C}}_{\widetilde{\underline{B}}}^* \underline{\mathfrak{C}}_{\underline{B}}$ to an eigenmatrix $U \in \mathbb{C}^{n \times m}$. Then $U \notin \ker(\underline{\mathfrak{C}}_{\underline{B}})$, hence $\underline{\mathfrak{C}}_{\underline{B}}(U)$ is a family of matrices, not all of which are the 0-matrix, and

$$\underline{\mathfrak{C}}_{\underline{B}} \underline{\mathfrak{C}}_{\widetilde{\underline{B}}}^* (\underline{\mathfrak{C}}_{\underline{B}}(U)) = \underline{\mathfrak{C}}_{\underline{B}} \underline{\mathfrak{C}}_{\widetilde{\underline{B}}}^* \underline{\mathfrak{C}}_{\underline{B}}(U) = \underline{\mathfrak{C}}_{\underline{B}}(\nu U) = \nu \underline{\mathfrak{C}}_{\underline{B}}(U),$$

making ν an eigenvalue of $\underline{\mathfrak{C}}_{\underline{B}} \underline{\mathfrak{C}}_{\underline{\tilde{B}}}^*$ to the eigenfamily of matrices $\underline{\mathfrak{C}}_{\underline{B}}(U)$.

Vice versa if $\nu \neq 0$ is an eigenvalue of $\underline{\mathfrak{C}}_{\underline{B}} \underline{\mathfrak{C}}_{\underline{\tilde{B}}}^*$ to an eigenfamily of matrices $\underline{W} \in \Gamma$, then in particular $\underline{W} \notin \ker(\underline{\mathfrak{C}}_{\underline{\tilde{B}}}^*)$, hence $\underline{\mathfrak{C}}_{\underline{\tilde{B}}}^*(\underline{W})$ is not the 0-matrix, and

$$\underline{\mathfrak{C}}_{\underline{\tilde{B}}}^* \underline{\mathfrak{C}}_{\underline{B}} \left(\underline{\mathfrak{C}}_{\underline{\tilde{B}}}^*(\underline{W}) \right) = \underline{\mathfrak{C}}_{\underline{\tilde{B}}}^* \underline{\mathfrak{C}}_{\underline{B}} \underline{\mathfrak{C}}_{\underline{\tilde{B}}}^*(\underline{W}) = \underline{\mathfrak{C}}_{\underline{\tilde{B}}}^*(\nu \underline{W}) = \nu \underline{\mathfrak{C}}_{\underline{\tilde{B}}}^*(\underline{W}) ,$$

making ν an eigenvalue of $\underline{\mathfrak{C}}_{\underline{\tilde{B}}}^* \underline{\mathfrak{C}}_{\underline{B}}$ to an eigenmatrix $\underline{\mathfrak{C}}_{\underline{\tilde{B}}}^*(\underline{W})$. In consequence this shows that all non-zero eigenvalues of $\underline{\mathfrak{C}}_{\underline{B}} \underline{\mathfrak{C}}_{\underline{\tilde{B}}}^*$ are given by (2.1), concluding the proof. \square

The proof of the following main theorem is postponed to Section 4.

Theorem 2.5. *Let $F \in \mathbb{R}^{n \times m}$, $\kappa \in \{1, 2\}$, $\beta \in \mathbb{R}_+$ and let $(A, \underline{B}, \underline{\tilde{B}}) \in \Gamma_{1+2P}$ be input filters with weakly factoring $(\underline{B}, \underline{\tilde{B}})$ satisfying the (CPC). Then, Problem 1.1 has a solution $(U^\dagger, \underline{W}^\dagger, \underline{\lambda}^\dagger) \in \Gamma_{1+2P}$.*

3 Previous Models Which Are Special Cases

In this section, first, for convenience, we briefly recall the connection between the classic ℓ^1 -regularized minimization problem (1.3) and the saddle point problem for the augmented Lagrangian which gave rise to the the AL/ADMM algorithm, on the one hand and our generalized AL/ADMM Algorithm 1.2 on the other hand.

Secondly, we reverse engineer the minimization problem (1.5), showing that it is a special case of Problem 1.1.

3.1 Classic ℓ^1 -Regularizations

Minimizing \mathcal{J}_{VAR} from (1.3) via differentiation poses a problem due to non-differentiability of the ℓ^1 -norm. As a workaround (see e.g. [WT10]) an equivalent constrained problem minimizing

$$\tilde{\mathcal{J}}_{\text{VAR}}(U, \underline{W}) = |\underline{W}|_{1, \kappa} + \frac{\mu}{2} \|U - F\|^2 , \text{ under the constraint } \underline{\mathfrak{C}}_{\underline{B}}(U) = \underline{W} , \quad (3.1)$$

is considered. To solve (3.1), for $\beta \in \mathbb{R}_+$ the augmented Lagrangian method computes the saddle point of the associated augmented Lagrangian functional,

$$\mathcal{J}_{\text{AL}}(U, \underline{W}, \underline{\lambda}) = |\underline{W}|_{1, \kappa} + \frac{\mu}{2} \|U - F\|^2 + \frac{\beta}{2} \|\underline{W} - \underline{\mathfrak{C}}_{\underline{B}}(U)\|^2 + \langle \underline{\lambda}, \underline{W} - \underline{\mathfrak{C}}_{\underline{B}}(U) \rangle , \quad (3.2)$$

i.e. the point $(U^\dagger, \underline{W}^\dagger, \underline{\lambda}^\dagger) \in \Gamma_{1+2P}$ satisfying

$$\mathcal{J}_{\text{AL}}(U^\dagger, \underline{W}^\dagger, \underline{\lambda}) \leq \mathcal{J}_{\text{AL}}(U^\dagger, \underline{W}^\dagger, \underline{\lambda}^\dagger) \leq \mathcal{J}_{\text{AL}}(U, \underline{W}, \underline{\lambda}^\dagger) , \quad (3.3)$$

for all $(U, \underline{W}, \underline{\lambda}) \in \Gamma_{1+2P}$. Notably, the saddle point is independent of the choice of $\beta \in \mathbb{R}_+$.

The AL/ADMM-algorithm computing the saddle point of (3.2) iterates the following steps: Minimize \mathcal{J}_{AL} over \underline{W} and U , for fixed $(U, \underline{\lambda})$ and $(\underline{W}, \underline{\lambda})$, respectively, and update $\underline{\lambda}$ via a gradient step.

Algorithm 3.1. For $\tau = 1, 2, \dots$ do

$$\begin{aligned}\underline{W}^{(\tau)} &= \arg \min_{\underline{W} \in \Gamma_P} \mathcal{J}_{\text{AL}} \left(U^{(\tau-1)}, \underline{W}, \underline{\lambda}^{(\tau)} \right), \\ U^{(\tau)} &= \arg \min_{U \in \mathbb{R}^{n \times m}} \mathcal{J}_{\text{AL}} \left(U, \underline{W}^{(\tau)}, \underline{\lambda}^{(\tau)} \right), \\ \underline{\lambda}^{(\tau+1)} &= \underline{\lambda}^{(\tau)} + \beta \left(\underline{W}^{(\tau)} - \underline{\mathfrak{C}}_{\underline{B}} \left(U^{(\tau)} \right) \right).\end{aligned}$$

For the convergence of Algorithm 3.1, where the ADMM part is approximately solved by performing only one iteration, see [GLT89][Th. 2.2] and [EB92][Th. 8]. In the special case of the $TV - \ell^2$ problem (1.4) see [WT10] for the equivalence of minimizing (1.3) and finding the saddle point for (3.2) as well as for a detailed proof of convergence of Algorithm 3.1 in the discrete case.

In every step of Algorithm 3.1 the two minimizers are explicitly given by (cf. Boyd and Vandenberg [BV04])

$$\begin{aligned}\underline{W}^{(\tau)} &= \mathfrak{S}_{\kappa} \left(\underline{\mathfrak{C}}_{\underline{B}} \left(U^{(\tau-1)} \right) - \frac{1}{\beta} \underline{\lambda}^{(\tau)}, \frac{1}{\beta} \right), \\ U^{(\tau)} &= \mu \left(\mu \mathfrak{E} + \beta \left(\underline{\mathfrak{C}}_{\underline{B}}^* \underline{\mathfrak{C}}_{\underline{B}} \right) \right)^{-1} (F) + \beta \left(\mu \mathfrak{E} + \beta \left(\underline{\mathfrak{C}}_{\underline{B}}^* \underline{\mathfrak{C}}_{\underline{B}} \right) \right)^{-1} \underline{\mathfrak{C}}_{\underline{B}}^* \left(\underline{W}^{(\tau)} + \frac{1}{\beta} \underline{\lambda}^{(\tau)} \right).\end{aligned}$$

Choosing filters A and filter families $\tilde{\underline{B}}$ determined by

$$\begin{aligned}\hat{A}[k, \ell] &= \mu \left(\mu + \beta \sum_{p=1}^P \left\| \hat{B}_p[k, \ell] \right\|^2 \right)^{-1}, \\ \hat{\tilde{B}}_p[k, \ell] &= \beta \left(\mu + \beta \sum_{q=1}^P \left\| \hat{B}_q[k, \ell] \right\|^2 \right)^{-1} \hat{B}_p[k, \ell],\end{aligned}$$

for $1 \leq p \leq P$, $0 \leq k \leq n-1$ and $0 \leq \ell \leq m-1$, verify that

$$\mathfrak{C}_A = \mu \left(\mu \mathfrak{E} + \beta \underline{\mathfrak{C}}_{\underline{B}}^* \underline{\mathfrak{C}}_{\underline{B}} \right)^{-1} \quad \text{and} \quad \underline{\mathfrak{C}}_{\tilde{\underline{B}}}^* = \beta \left(\mu \mathfrak{E} + \beta \underline{\mathfrak{C}}_{\underline{B}}^* \underline{\mathfrak{C}}_{\underline{B}} \right)^{-1} \underline{\mathfrak{C}}_{\underline{B}}^*. \quad (3.4)$$

Thus, we arrive at a special case of Problem 1.1.

Problem 3.2. Find a point $(U^\dagger, \underline{W}^\dagger, \underline{\lambda}^\dagger) \in \Omega_1^k \cap \Omega_2 \cap \Omega_C$ where

$$\begin{aligned}\Omega_1^k &:= \left\{ (U, \underline{W}, \underline{\lambda}) \in \Gamma_{1+2P} : \underline{W} = \mathfrak{S}_{\kappa} \left(\underline{\mathfrak{C}}_{\underline{B}} (U) - \frac{1}{\beta} \underline{\lambda}; \frac{1}{\beta} \right) \right\}, \\ \Omega_2 &:= \left\{ (U, \underline{W}, \underline{\lambda}) \in \Gamma_{1+2P} : \right. \\ &\quad \left. U = \mu \left(\mu \mathfrak{E} + \beta \underline{\mathfrak{C}}_{\underline{B}}^* \underline{\mathfrak{C}}_{\underline{B}} \right)^{-1} (F) + \beta \left(\mu \mathfrak{E} + \beta \underline{\mathfrak{C}}_{\underline{B}}^* \underline{\mathfrak{C}}_{\underline{B}} \right)^{-1} \underline{\mathfrak{C}}_{\underline{B}}^* \left(\underline{W} + \frac{1}{\beta} \underline{\lambda} \right) \right\}, \\ \Omega_C &:= \left\{ (U, \underline{W}, \underline{\lambda}) \in \Gamma_{1+2P} : \underline{\mathfrak{C}}_{\underline{B}} (U) = \underline{W} \right\}.\end{aligned} \quad (3.5)$$

As in the introduction, we have at once the analogue of Remark 1.3.

Remark 3.3. *Problem 3.2 is a special case of Problem 1.1. Furthermore, every intersection point of Problem 3.2 is a fixed point of Algorithm 3.1 and vice versa.*

3.2 The Generalized Hilbert Model

Replacing the ℓ^2 -norm in the data-fidelity term of (1.4) with a more flexible Hilbert norm one arrives at (1.5), as proposed for $\underline{\mathfrak{C}}_{\underline{B}} = \nabla$ by Aujol and Gilboa [AG06]. It turns out that the corresponding minimization problem is also a special case of Problem 1.1, and *strongly factoring* filters from Definition 2.2 (ii) assure equivalence.

Theorem 3.4. *For $F \in \mathbb{R}^{n \times m}$, $\underline{B} \in \Gamma_P$ and $\kappa \in \{1, 2\}$ the following hold:*

- (i) *If $U^\dagger \in \Gamma$ is a minimizer of (1.5) for some $\mu \in \mathbb{R}_+$ and $M \in \mathbb{R}^{n \times m}$ such that $\widehat{M} \in \mathbb{R}_+^{n \times m}$, then there are $\beta \in \mathbb{R}_+$, $A \in \mathbb{R}^{n \times m}$ and a strong factor matrix $Y \in \mathbb{R}^{n \times m}$ yielding $\widetilde{B} \in \Gamma_P$ from \underline{B} such that $(\underline{B}, \widetilde{B})$ satisfy the (CPC) and, with suitable $(\underline{W}^\dagger, \underline{\lambda}^\dagger) \in \Gamma_{2P}$, $(U^\dagger, \underline{W}^\dagger, \underline{\lambda}^\dagger)$ is a solution of Problem 1.1.*
- (ii) *If $(U^\dagger, \underline{W}^\dagger, \underline{\lambda}^\dagger) \in \Gamma_{1+2P}$ is a solution of Problem 1.1 with $\kappa \in \{1, 2\}$, $\beta \in \mathbb{R}_+$ and $(A, \underline{B}, \widetilde{B}) \in \Gamma_{1+2P}$ with strongly factoring $(\underline{B}, \widetilde{B})$ satisfying the (CPC), then there are $\mu \in \mathbb{R}_+$ and $M \in \mathbb{R}^{n \times m}$ with $\widehat{M} \in \mathbb{R}_+^{n \times m}$ such that U^\dagger is a minimizer of (1.5).*

Proof. (i): With the argument detailed in Section 3.1, for every minimizer $U^\dagger \in \Gamma$ of (1.5) there are $(\underline{W}^\dagger, \underline{\lambda}^\dagger) \in \Gamma_{2P}$ such that $(U^\dagger, \underline{W}^\dagger, \underline{\lambda}^\dagger)$ solves an AL problem similar to (3.3) and a corresponding saddle point equation similar to (3.3). Then [RTGH, Theorem 7.4, first assertion] asserts the existence of a strong factor $Y \in \Gamma$ yielding $\widetilde{B} \in \Gamma_P$ from \underline{B} such that $(U^\dagger, \underline{W}^\dagger, \underline{\lambda}^\dagger)$ solves Problem 1.1.

(ii): From Lemma 2.4 infer that $\underline{\mathfrak{C}}_{\underline{B}}^* \underline{\mathfrak{C}}_{\underline{B}}$ has non-negative eigenvalues, which, in case of (CPC), are then in $[0, 1)$. In consequence of [RTGH, Theorem 7.4, second assertion] there are suitable $\mu \in \mathbb{R}_+$ and $M \in \mathbb{R}^{n \times m}$ with $\widehat{M} \in \mathbb{R}_+^{n \times m}$ such that U^\dagger is a minimizer of (1.5). \square

Remark 3.5. (i) *The functional \mathcal{J}_{HIL} of (1.5) is strictly convex, coercive and lower semi-continuous, yielding the existence of a unique minimizer. Moreover, its AL/ADMM-algorithm is Algorithm 1.2 which convergences by virtue of Eckstein and Bertsekas [EB92][Theorem 8].*

- (ii) *Theorem 3.4 can be extended to feature strongly factoring $(\underline{B}, \widetilde{B})$ that only satisfy the (NEPC) when allowing the entries of \widehat{M} to be in $\mathbb{R}_+ \cup \{0\}$. In this case a minimizer is not necessary unique, since \mathcal{J}_{HIL} is not necessary strongly convex.*

4 Proof of the Main Theorem

For $\kappa = 1, 2$ consider the set valued functions

$$\begin{aligned} \Upsilon^\kappa : \mathbb{R}^{n \times m} &\rightrightarrows \Gamma_P, \\ U &\mapsto \left\{ \underline{\lambda} \in \Gamma_P : 0 \in \partial|_{\underline{W}=\underline{\mathfrak{C}}_{\underline{B}}(U)} \left(|\underline{W}|_{1,\kappa} + \langle \underline{\lambda}, \underline{W} \rangle \right) \right\}. \end{aligned} \quad (4.1)$$

Here, $\partial|_{\underline{W}=\underline{\mathfrak{C}}_{\underline{B}}(U)}$ denotes the set valued subdifferential (e.g. [BC11]) of a convex function with respect to \underline{W} evaluated at $\underline{\mathfrak{C}}_{\underline{B}}(U)$. Defining $\Omega_S^\kappa := \text{graph}(\Upsilon^\kappa)$ we

have,

$$\Omega_S^1 = \left\{ (U, \underline{\lambda}) \in \Gamma_{1+P} : \lambda_p[k, \ell] \begin{cases} = -1 & \text{if } \mathfrak{C}_{B_p}(U)[k, \ell] > 0 \\ \in [-1, 1] & \text{if } \mathfrak{C}_{B_p}(U)[k, \ell] = 0 \\ = 1 & \text{if } \mathfrak{C}_{B_p}(U)[k, \ell] < 0 \end{cases}, \text{ for all } k, \ell, p \right\}, \quad (4.2)$$

and

$$\Omega_S^2 = \left\{ (U, \underline{\lambda}) \in \Gamma_{1+P} : (\lambda_p[k, \ell])_{p=1}^P \begin{cases} = -\frac{(\mathfrak{C}_{B_p}(U)[k, \ell])_{p=1}^P}{\|(\mathfrak{C}_{B_p}(U)[k, \ell])_{p=1}^P\|} & \text{if } \|(\mathfrak{C}_{B_p}(U)[k, \ell])_{p=1}^P\| > 0 \\ \in \mathcal{K}_1(0) & \text{if } \|(\mathfrak{C}_{B_p}(U)[k, \ell])_{p=1}^P\| = 0 \end{cases}, \text{ for all } k, \ell \right\}, \quad (4.3)$$

where $\mathcal{K}_1(0)$ is the closed unit ball around the origin. We also need the following set,

$$\Omega_F^G := \left\{ (U, \underline{\lambda}) \in \Gamma_{1+P} : U = \left(\mathfrak{C} - \underline{\mathfrak{C}}_{\underline{B}}^* \underline{\mathfrak{C}}_{\underline{B}} \right)^{-1} \mathfrak{C}_A(F) + \frac{1}{\beta} \left(\mathfrak{C} - \underline{\mathfrak{C}}_{\underline{B}}^* \underline{\mathfrak{C}}_{\underline{B}} \right)^{-1} \underline{\mathfrak{C}}_{\underline{B}}^*(\underline{\lambda}) \right\},$$

which is well defined in case the (CPC) holds as proof of Lemma 4.1 teaches. In order to prove Theorem 2.5 we need to show that $\Omega_1^\kappa \cap \Omega_2^G \cap \Omega_C \neq \emptyset$. The following Lemma asserts that we can equivalently show that $\Omega_F^G \cap \Omega_S^\kappa \neq \emptyset$.

Lemma 4.1. *Let $F \in \mathbb{R}^{n \times m}$, $\beta \in \mathbb{R}_+$ and $(A, \underline{B}, \tilde{\underline{B}}) \in \Gamma_{1+2P}$ with weakly factoring $(\underline{B}, \tilde{\underline{B}})$ satisfying the (CPC). Then $(U, \underline{\lambda}) \in \Omega_F^G \cap \Omega_S^\kappa$ if and only if there exists $\underline{W} \in \Gamma_P$ such that $(U, \underline{W}, \underline{\lambda}) \in \Omega_1^\kappa \cap \Omega_2^G \cap \Omega_C$.*

Proof. As shown in Lemma 2.4, if $(\underline{B}, \tilde{\underline{B}})$ factors weakly, then $\underline{\mathfrak{C}}_{\underline{B}}^* \underline{\mathfrak{C}}_{\underline{B}}$ diagonalizes and in conjunction with (CPC), all eigenvalues are non-negative and strictly less than one. In consequence, $\mathfrak{C} - \underline{\mathfrak{C}}_{\underline{B}}^* \underline{\mathfrak{C}}_{\underline{B}}$ is invertible and hence

$$U = \left(\mathfrak{C} - \underline{\mathfrak{C}}_{\underline{B}}^* \underline{\mathfrak{C}}_{\underline{B}} \right)^{-1} \mathfrak{C}_A(F) + \frac{1}{\beta} \left(\mathfrak{C} - \underline{\mathfrak{C}}_{\underline{B}}^* \underline{\mathfrak{C}}_{\underline{B}} \right)^{-1} \underline{\mathfrak{C}}_{\underline{B}}^*(\underline{\lambda})$$

is equivalent with

$$U - \underline{\mathfrak{C}}_{\underline{B}}^*(\underline{W}) = \mathfrak{C}_A(F) + \frac{1}{\beta} \underline{\mathfrak{C}}_{\underline{B}}^*(\underline{\lambda})$$

yielding

$$(U, \underline{W}, \underline{\lambda}) \in \Omega_2^G \cap \Omega_C \Leftrightarrow (U, \underline{\lambda}) \in \Omega_F^G.$$

Further, by definition we have at once that $(U, \underline{\lambda}) \in \Omega_S^\kappa$ implies that $(U, \underline{W}, \underline{\lambda}) \in \Omega_1^\kappa$ for all $\underline{W} \in \Gamma_P$. Vice versa, if $\underline{W} = \underline{\mathfrak{C}}_{\underline{B}}(U)$, then verify that the inverse statement, $(U, \underline{W}, \underline{\lambda}) \in \Omega_1^\kappa$ implies that $(U, \underline{\lambda}) \in \Omega_S^\kappa$, is also true. \square

Next, we show that

$$\Omega_S^0 := \{ (U, \underline{\lambda}) \in \Gamma_{1+P} : \underline{\lambda} = \underline{0} \}. \quad (4.4)$$

is an affine complement of the affine space $\Omega_F^G \subset \Gamma_{1+P}$.

Lemma 4.2. *Let $F \in \mathbb{R}^{n \times m}$, $\beta \in \mathbb{R}_+$ and $(A, \underline{B}, \tilde{\underline{B}}) \in \Gamma_{1+2P}$ with weakly factoring $(\underline{B}, \tilde{\underline{B}})$ satisfying the (CPC). Then*

$$\Omega_S^0 \oplus \Omega_F^G = \Gamma_{1+P}.$$

Proof. As argued in the proof of Lemma 4.1, weakly factoring filters satisfying the (CPC) imply that $\mathfrak{E} - \underline{\mathfrak{C}}_{\tilde{\underline{B}}}^* \underline{\mathfrak{C}}_{\underline{B}}$ is invertible and thus

$$\left(\left(\mathfrak{E} - \underline{\mathfrak{C}}_{\tilde{\underline{B}}}^* \underline{\mathfrak{C}}_{\underline{B}} \right)^{-1} \mathfrak{C}_{A(F), \underline{0}} \right) \in \Omega_S^0 \cap \Omega_F^G.$$

To see uniqueness suppose $(U_1, \lambda_1), (U_2, \lambda_2) \in \Omega_S^0 \cap \Omega_F^G$. Then $\lambda_1 = 0 = \lambda_2$ yielding,

$$U_1 - U_2 = \frac{1}{\beta} \left(\mathfrak{E} - \underline{\mathfrak{C}}_{\tilde{\underline{B}}}^* \underline{\mathfrak{C}}_{\underline{B}} \right)^{-1} \underline{\mathfrak{C}}_{\tilde{\underline{B}}}^* (\lambda_1 - \lambda_2) = 0.$$

The dimension of Ω_S^0 is nm , while that of Ω_F^G is Pnm as being the graph of a linear function from Γ_P to $\mathbb{R}^{n \times m}$. Since we just showed $\dim(\Omega_S^0 \cap \Omega_F^G) = 0$, we have indeed $\Omega_S^0 \oplus \Omega_F^G = \Gamma_{1+P}$. \square

In the following, let $U_0 \in \mathbb{R}^{n \times m}$ give rise to the unique intersection point

$$(U_0, \underline{0}) \in \Omega_S^0 \cap \Omega_F^G \tag{4.5}$$

guaranteed by Lemma 4.2.

Further let $\theta \in (0, \pi/2]$ denote the *first principal angle* between $\Omega_S^0 \cap \Omega_F^G$. In general for two affine subspaces $\Xi, \Omega \subset \mathbb{R}^D$, each of positive dimension, with unique intersection point $v \in \Xi \cap \Omega$, the first principle angle between Ξ and Ω is defined by

$$\max_{\substack{\xi + v \in \Xi : \|\xi\| = 1 \\ \omega + v \in \Omega : \|\omega\| = 1}} (\xi^T \omega)^2 = \cos^2(\theta) \in [0, 1),$$

cf. [Jor75]. We need the following estimate in the additional case of $\mathbb{R}^D = \Xi \oplus \Omega$, the proof of which is deferred to the appendix.

Lemma 4.3. *With the above assumptions and notations suppose that $\phi : \Omega \rightarrow \mathbb{R}^D$ is continuous, satisfying*

$$\|\phi(\omega) - \omega\| \leq C, \text{ for all } \omega \in \Omega,$$

for a constant $C > 0$. Then $\Xi \cap \phi(\Omega) \neq \emptyset$ and

$$\|u - v\| \leq C \left(1 + \frac{1}{\sin(\theta)} \right),$$

for all $u \in \Xi \cap \phi(\Omega)$.

In application of Lemma 4.3, set $C := Pnm + 1$ and $R := C(1 + 1/\sin(\theta))$ to obtain the compact ball

$$\mathcal{K} := \{U \in \mathbb{R}^{n \times m} : \|U - U_0\| \leq R\},$$

around U_0 .

In the next step, we approximate Y^κ by a single-valued function v_r^κ , $r > 0$, in order to consider $r \rightarrow 0$ afterwards. We use the *separation of P from Q*

$$d(P, Q) := \sup_{p \in P} \left(\inf_{q \in Q} (\|p - q\|) \right),$$

for $P, Q \subset \mathbb{R}^D$, cf. [Cel69].

Lemma 4.4. *For every $r > 0$ there is a continuous mapping $v_r^\kappa : \mathcal{K} \rightarrow \Gamma_{1+P}$ such that $d(\text{graph}(v_r^\kappa), \text{graph}(Y^\kappa|_{\mathcal{K}})) \leq r$.*

Proof. By definition, cf. (4.2) and (4.3), the functions Y^κ are convex valued (i.e. $Y^\kappa(U)$ is a convex set for every $U \in \mathbb{R}^{n \times m}$) and their graphs Ω_S^κ are closed (due to continuity of $\underline{\mathfrak{C}}_B$). Since they map to convex subsets of a compact set, they are upper semi-continuous (e.g. [Cel69][p. 19]). Thus [Cel69][Theorem 1] is applicable, yielding the existence of v_r^κ . \square

With $v_r := v_r^\kappa$ (for ease of notation dropping the superscript κ) from Lemma 4.4, we have thus that for every $U \in \mathcal{K}$ there are $U' \in \mathcal{K}$ and $\underline{\lambda}' \in Y^\kappa(U')$ such that

$$\|U - U'\|^2 + \|v_r(U) - \underline{\lambda}'\|^2 \leq r^2.$$

Since $\|\underline{\lambda}'\|^2 \leq Pnm$ by definition of Y^κ in (4.2) and (4.3), we have

$$\|v_r(U)\| \leq Pnm + 1 \text{ for all } U \in \mathcal{K} \text{ and } r < 1.$$

In consequence, the single-valued, continuous mapping

$$\phi_r : \Omega_S^0 \rightarrow \Gamma_{1+P}, \quad (U, \underline{0}) \mapsto (U, v_r(\mathcal{P}_{\mathcal{K}}(U))),$$

where $\mathcal{P}_{\mathcal{K}}$ is the orthogonal projection of $\mathbb{R}^{n \times m}$ onto \mathcal{K} , satisfies

$$\|\phi_r(\omega) - \omega\| \leq Pmn + 1 = C.$$

Since $(U_0, \underline{0})$ is the unique intersection point of Ω_S^0 and Ω_F^G , cf. (4.5) and Lemma 4.2, application of Lemma 4.3 yields for all $0 < r < 1$ the existence of $(U_r, \underline{\lambda}_r) \in \Omega_F^G \cap \phi_r^\kappa(\Omega_S^0)$ with the property

$$\|(U_r, \underline{\lambda}_r) - (U_0, \underline{0})\| \leq (Pmn + 1) \left(1 + \frac{1}{\sin \theta} \right).$$

We conclude that $U_r \in \mathcal{K}$ and hence $\underline{\lambda}_r = v_r(U_r)$. Moreover, since the sequence $(U_r, \underline{\lambda}_r) \in \text{graph}(v_r)$ ($r = 1/n, n \in \mathbb{N}$) is bounded, it has a cluster point $(U^\dagger, \underline{\lambda}^\dagger) \in \Omega_F^G$ because Ω_F^G is closed. Further, since $d(\text{graph}(v_r), \text{graph}(Y^\kappa)) \rightarrow 0$ with respect to the separation d , $(U^\dagger, \underline{\lambda}^\dagger)$ is in the closure of $\text{graph}(Y^\kappa) = \Omega_S^\kappa$, which is closed, as remarked above in the proof of Lemma 4.4. Hence

$$(U^\dagger, \underline{\lambda}^\dagger) \in \Omega_F^G \cap \Omega_S^\kappa,$$

yielding the assertion of Theorem 2.5, due to Lemma 4.1.

5 Numerical Experiments

In illustration of the potential of our generalized algorithm we consider two classic problems in image decomposition: denoising and cartoon-texture decomposition. As proof of concept we show that ad-hoc filters yield results comparable or even better than classical filters. Subjecting such filters to methods learning over larger classes is beyond the scope of this work and left for future research.

5.1 Building New Filters for Denoising

We illustrate how new (weakly or strongly) factoring filters can be easily obtained from existing models, that, as they feature more parameters, outperform existing models. To this end, we consider four classic test images $U \in \mathbb{R}^{n \times m}$ (taken from [gra]) listed in Table 2 with additive Gaussian noise ϵ ,

$$F = U + \epsilon, \text{ where } \epsilon \sim \mathcal{N}(0, \mathfrak{C}_{Z_x} \mathfrak{C}_{Z_x}^*),$$

correlated in horizontal direction,

$$Z_x = \frac{\sqrt{50}}{20} \begin{pmatrix} 4 & 4 & 2 & 1 & 0 & \cdots & 0 & 1 & 2 & 4 \\ 1 & 0 & 0 & 0 & 0 & & & 0 & 0 & 0 \\ 0 & 0 & \ddots & & & & & & 0 & 0 \\ \vdots & & & & & & & & & \vdots \\ 0 & 0 & & & & & & \ddots & & 0 \\ 1 & 0 & \cdots & & & & \cdots & 0 & 0 \end{pmatrix}.$$

We compare three models for denoising and for each image we perform 100 experiments and record their respective peak signal to noise ratio (PSNR) mean \pm standard deviation in Table 2. In all 100 experiments the PSNR of Models II and III outperformed the PSNR of Model I.

Model I: classical $TV - \ell^2$. As illustrated in (3.4), denoting by $\underline{D} \in \Gamma^2$ the filters yielding the discrete derivative operator, i.e. $\nabla = \underline{\mathfrak{C}}_{\underline{D}}$, in this model we have

$$\underline{\mathfrak{C}}_{\underline{B}} = \underline{\mathfrak{C}}_{\underline{D}} \text{ and } \underline{\mathfrak{C}}_{\underline{B}}^* = \mathfrak{C}_Y \underline{\mathfrak{C}}_{\underline{B}}^* \quad \text{where} \quad \mathfrak{C}_Y = \beta \left(\mu \mathfrak{E} + \beta \underline{\mathfrak{C}}_{\underline{B}}^* \underline{\mathfrak{C}}_{\underline{B}} \right)^{-1}, \quad (5.1)$$

as well as $\mathfrak{C}_A = \mu \left(\mu \mathfrak{E} + \beta \underline{\mathfrak{C}}_{\underline{B}}^* \underline{\mathfrak{C}}_{\underline{B}} \right)^{-1}$ where $\mu > 0$ is the one weight optimized over.

Model II: strongly factoring with spectrally weighted gradient coordinates. Inspired from (5.1) we place different weights on the spectral coordinates of the derivative operator via

$$\underline{\mathfrak{C}}_{\underline{B}} = \underline{\mathfrak{C}}_{\underline{D}} \mathfrak{C}_V \text{ and } \mathfrak{C}_Y = \beta \left(\mu \mathfrak{E} + \beta \underline{\mathfrak{C}}_{\underline{B}}^* \underline{\mathfrak{C}}_{\underline{B}} \right)^{-1} \mathfrak{C}_V^2$$

where

$$\widehat{V}[k, \ell] := \exp(-y_1 \omega_k^2 - y_2 \omega_\ell^2) = \widehat{V}[k, \ell]^{-1}, \quad 0 \leq k \leq n-1 \text{ and } 0 \leq \ell \leq m-1$$

Table 1

Trained parameters; μ has not been trained for Models II and III but the optimal values from Model I have been used.

Image	Model I	Model II		Model III	
	μ	y_1	y_2	r_1	r_2
barbara	0.0818	-0.07	0.042	0.7408	1.3499
cameraman	0.054	-0.07	0.014	0.7408	1.3499
boat	0.051	-0.07	0.014	0.7408	1.3499
goldhill	0.0458	-0.07	0.014	0.7408	1.1972

and

$$\omega_k := \begin{cases} \frac{2\pi k}{n} & \text{if } k < \frac{n}{2} \\ -2\pi + \frac{2\pi k}{n} & \text{else} \end{cases} \quad \text{and} \quad \omega_\ell := \begin{cases} \frac{2\pi \ell}{m} & \text{if } \ell < \frac{m}{2} \\ -2\pi + \frac{2\pi \ell}{m} & \text{else} \end{cases}, \quad (5.2)$$

such that $\underline{\mathfrak{C}}_{\underline{B}}^* = \underline{\mathfrak{C}}_Y \underline{\mathfrak{C}}_{\underline{B}}^* = \beta \left(\mu \underline{\mathfrak{C}} + \beta \underline{\mathfrak{C}}_{\underline{D}}^* \underline{\mathfrak{C}}_{\underline{D}} \right)^{-1} \underline{\mathfrak{C}}_{\underline{V}} \underline{\mathfrak{C}}_{\underline{D}}^*$, cf. Remark 2.3. With $\underline{\mathfrak{C}}_A$ unchanged, by definition, we arrive at a strongly factoring model with three weights μ, y_1, y_2 optimized over.

Model III: weakly factoring with spectrally weighted gradient directions. Now, taking $Y^{TV-\ell^2}$ from the classical $TV - \ell^2$ -model above in (5.1) with $\underline{\mathfrak{C}}_{Y^{TV-\ell^2}} = \beta \left(\mu \underline{\mathfrak{C}} + \beta \underline{\mathfrak{C}}_{\underline{B}}^* \underline{\mathfrak{C}}_{\underline{B}} \right)^{-1}$ and defining

$$\underline{\mathfrak{C}}_{Y^{TV-\ell^2}} : \Gamma_P \rightarrow \Gamma_P, \underline{H} \mapsto \left(\underline{\mathfrak{C}}_{Y^{TV-\ell^2}}(H_1), \dots, \underline{\mathfrak{C}}_{Y^{TV-\ell^2}}(H_P) \right),$$

we place different weights on the spectral representation of the directional derivatives via

$$\underline{\mathfrak{C}}_{\underline{B}} = \underline{\mathfrak{C}}_{\underline{R}} \underline{\mathfrak{C}}_{\underline{D}} \quad \text{and} \quad \underline{\mathfrak{C}}_{\underline{Y}} = \underline{\mathfrak{C}}_{Y^{TV-\ell^2}} \underline{\mathfrak{C}}_{\underline{R}}^2$$

where $\underline{R} = (R_1, R_2) \in \Gamma^2$ with

$$\widehat{R}_1[k, \ell] := r_1 =: \widehat{R}_1[k, \ell]^{-1} \quad \text{and} \quad \widehat{R}_2[k, \ell] := r_2 =: \widehat{R}_2[k, \ell]^{-1}, \quad r_1, r_2 > 0,$$

for all $0 \leq k \leq n-1$ and $0 \leq \ell \leq m-1$, such that

$$\underline{\mathfrak{C}}_{\underline{B}}^* = \underline{\mathfrak{C}}_{\underline{B}}^* \underline{\mathfrak{C}}_{\underline{Y}} = \beta \left(\mu + \beta \underline{\mathfrak{C}}_{\underline{D}}^* \underline{\mathfrak{C}}_{\underline{D}} \right)^{-1} \underline{\mathfrak{C}}_{\underline{D}}^* \underline{\mathfrak{C}}_{\underline{R}},$$

cf. Remark 2.3. With $\underline{\mathfrak{C}}_A$ unchanged, by definition, we arrive at a weakly factoring model with three weights μ, r_1, r_2 optimized over. Whenever $r_1 \neq r_2$ this model is not strongly factoring.

Model training. The model unspecific parameters are set to $\beta = 0.1$ and $\kappa = 2$, while we compute the solution of Problem 1.1 with Algorithm 1.2 up to accuracy $\epsilon = 10^{-5}$. For Model I, this accuracy was reached well before 500 iterations, for some of the runs for Models II and III after 500 iterations only an accuracy of $\epsilon = 10^{-4}$ has been reached. While μ has been optimized via bisection, the parameters r_1, r_2 and y_1, y_2 have been optimized via a grid search, cf. [Ric19].

Table 2

Peak signal to noise ratio (PSNR): mean \pm standard deviation from one hundred experiments each with underlined best mean PSNR and **bold** mean PSNR exceeding the mean PSNR of Model I ($TV - \ell^2$) by more than 0.1.

Image	PSNR		
	Model I	Model II	Model III
barbara	25.1158 \pm 0.0251	25.4197 \pm 0.0266	<u>25.5282 \pm 0.0257</u>
cameraman	26.8547 \pm 0.0664	27.0461 \pm 0.0582	<u>27.0957 \pm 0.0689</u>
boat	27.0946 \pm 0.0296	27.2183 \pm 0.0273	<u>27.3681 \pm 0.0303</u>
goldhill	27.4352 \pm 0.0322	27.4956 \pm 0.0326	<u>27.5305 \pm 0.0328</u>

5.2 A Laplace-Spline-Riesz Model Separating Cartoon and Texture

As another illustration of our approach, we now build an elaborate filter family separating cartoon and texture. Consider the *isotropic polyharmonic B-splines* which, for $\gamma \geq 1/2$, are given in the frequency domain by

$$\widehat{f}_\gamma(x, y) := \left(\frac{4 \left(\sin^2 \left(\frac{x}{2} \right) + \sin^2 \left(\frac{y}{2} \right) \right) - \frac{8}{3} \left(\sin \left(\frac{x}{2} \right) \sin \left(\frac{y}{2} \right) \right)}{(x^2 + y^2)} \right)^{\frac{\gamma}{2}}. \quad (5.3)$$

Van de Ville et al. [VDVBU05] explain how these splines are basis-splines (B-splines) for the discrete fractional Laplace operator $(\underline{\mathfrak{C}}_D^* \underline{\mathfrak{C}}_D)^\gamma$, and how, using (5.3) as the scaling function, a bi-orthogonal wavelet basis is constructed, drawing on a similar relation as between the Haar wavelet frame and the discrete gradient (see for example Cai et al. [CDOS12]). Using dyadic subsampling in the construction of the wavelet frame operators yields 3 wavelets per scale. We consider in this example $J+1 = 4$ scales to derive the high-pass filter pair $(\underline{B}, \widetilde{B})$. Additionally, we let $(\underline{B}, \widetilde{B})$ involve Riesz transforms with $Z = 3$ directions, cf. [USVDV09, UVDV10], giving in total families with $P = 3Z(J+1) = 36$ members. All of this is detailed in Appendix 9.

With the *autocorrelation function*

$$a_\gamma(x, y) := \sum_{r, s \in \mathbb{Z}} (f_\gamma(x + 2\pi r, y + 2\pi s))^2, \quad (5.4)$$

we obtain a low-pass filter A determined by

$$\widehat{A}[k, \ell] := \left\| \frac{f_\gamma(2^J \omega_k, 2^J \omega_\ell)}{\sqrt{a_\gamma(2^J \omega_k, 2^J \omega_\ell)}} \right\|^2,$$

with ω_k, ω_ℓ taken from (5.2). As detailed in Appendix 9, the resulting model is weakly factoring, it does not satisfy the (NEPC), however (some eigenvalues of $\underline{\mathfrak{C}}_{\widetilde{B}}^* \underline{\mathfrak{C}}_{\underline{B}}$ exceed 1). To this end, introduce $(0 \leq j \leq J, 1 \leq z \leq Z, 1 \leq s \leq 3)$

$$H[k, \ell] = \left(\widehat{A}[k, \ell] + \sum_{j, z, s} \overline{\widetilde{B}_{j, z, s}[k, \ell]} \widehat{B}_{j, z, s}[k, \ell] \right)^{-\frac{1}{2}},$$

to obtain the corrected matrix families

$$\widehat{A}^{\text{cor}} := H \odot H \odot \widehat{A}, \quad \widehat{B}_{(j,z,s)}^{\text{cor}} := H \odot \widehat{B}_{(j,z,s)}, \quad \widetilde{B}_{(j,z,s)}^{\text{cor}} := H \odot \widetilde{B}_{(j,z,s)}. \quad (5.5)$$

Then, the weakly factoring model resulting (with an additional minor adjustment leading to $\underline{B}^{\text{adj}}, \widetilde{B}^{\text{adj}}$, detailed in Appendix 9) from $(A^{\text{cor}}, \underline{B}^{\text{adj}}, \widetilde{B}^{\text{adj}})$ satisfies (numerically verified) the (CPC) and we call it the *Laplace-spline-Riesz* (LsR) model. We compare it to the $TV - \ell^2$ -model, cf. (1.4), the *OSV*-model ([OSV03], as an approximation of the $TV - G$ -model) and the TV -Hilbert model ((1.5) with $\underline{B} = \underline{D}$ and M as detailed in [BLMV10][Eq.8]).

Since there is no benchmarking available for cartoon-texture decomposition, in Figures 1 and 2 we inspect desirable features of resulting cartoons from five classic images from [gra], zooming in on specific details; for the complete set of cartoons obtained see Figures 3 and 4 in Appendix 10. We have manually chosen parameters (see Table 3) for each model, respectively, in order to remove all texture (specifically from the table cloth) from the "barbara" image (first column of Figure 1) while keeping all "large-scale" structures (specifically the upper edge separating the table cloth from the floor behind).

Model	κ	μ	β	$1/(2\pi\sigma)^4$	γ
$TV - \ell^2$	2	0.02	1	-	-
<i>OSV</i>	2	0.01	1	-	-
TV -Hilbert	2	0.125	1	0.125	-
LsR	1	-	1	-	1.2

Table 3: *Parameters to remove texture while keeping contrast (for the definition of σ see [BLMV10][Eq.8]). While in the first three models the choice of β has no effect on the solution, in the LsR model it does.*

While $TV - \ell^2$ and *OSV* retain some texture, especially along edges, (Figures 1 (d) and (h) as well as Figures 2 (d) and (h)), edges are sharper for TV -Hilbert and LsR (Figures 1 (l) and (p) as well as Figures 2 (j) and (m)). The same effects are visible in Column 3 of Figure 1. For LsR this comes at a price of slight blurring and light artefacts between the dark squares (Figure 1, (r)). On the other hand, the irregular water pattern (Column 4 of Figure 1) is only fully removed by LsR (Figure 1, (s)). Notably, only $TV - \ell^2$ was not able to remove all texture from the table cloth without losing the contrast between the upper edge of the table cloth and the floor behind (Figure 1, (d)). Similarly only $TV - \ell^2$ loses the contrast between the middle and bottom part of the sail (Figure 2, (e)). Finer scale texture patterns on the fish (Column 3 of Figure 2) are again fully removed only by LsR ((Figure 1, (r)).

Figures 1 and 2 show that the weakly factoring LsR filters lead to results comparable in texture removal to classic models in the literature. Since the LsR filters come with higher flexibility (e.g. the additional parameter $\gamma > \frac{1}{2}$ and the number of scales can be increased), they have the potential to be better trained for a specific task.

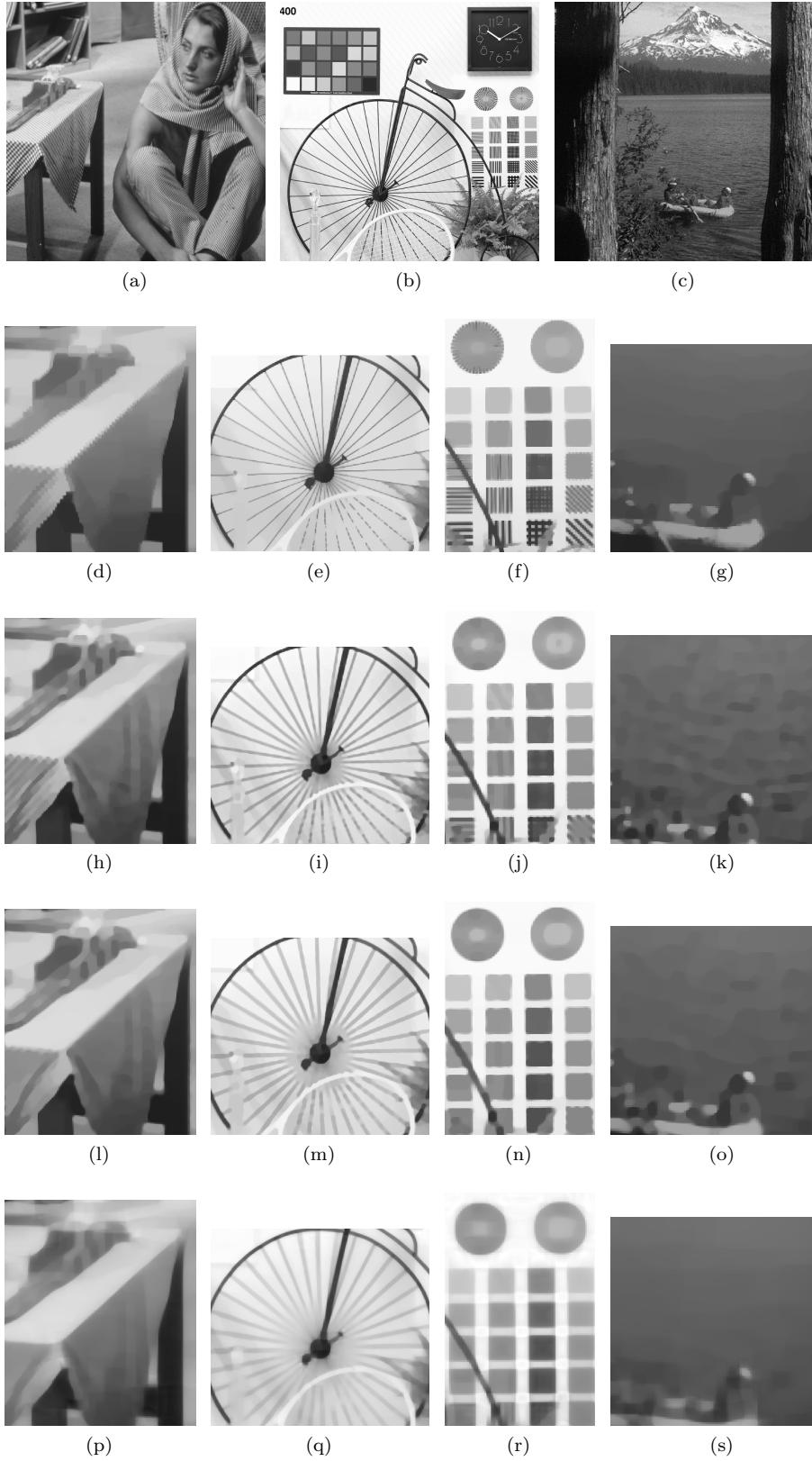


Figure 1: *Test images from [gra] (1st row): barbara (a), bicycle (b), lake (c). Enlarged details from cartoons computed via $TV - \ell^2$ (2nd row), OSV (3rd row), TV-Hilbert (4th row) and our LsR-model (5th row).*



(a)

(b)

(c)



(d)

(e)

(f)



(g)

(h)

(i)



(j)

(k)

(l)



(m)

(n)

(o)

Figure 2: Test images from [gra] (1st row): clutter (a), sail (b), fish. Enlarged details from cartoons computed via $TV - \ell^2$ (2nd row), $TV - G$ (3rd row), TV -Hilbert (4th row) and our LsR -model (5th row).

6 Outlook

In this paper we have introduced a general intersection point problem which features a solution under (CPC) and weakly factoring filters. We have explored some consequences of these conditions. It is an open problem whether additional conditions are necessary to establish convergence and to obtain a unique intersection point. Both of which are granted if weakly factoring is replaced with strongly factoring. For the weakly factoring filter families introduced, we have observed numerical convergence for all of the test images considered.

The weakly factoring filters satisfying the (CPC), introduced, serve as a proof of concept. Due to their broad range of parameters, they can be used for (deep) learning the goals of denoising and cartoon-texture decomposition, as we have touched in our applications. In particular when a loss-function for a specific task is available, minimizing this loss over a larger class of problems is desirable.

In current research we use the filters proposed in our applications as initial parameters that are fed into learning architectures, where filter families \underline{B} and corresponding factor families \underline{Y} are optimized over for supervised and unsupervised learning.

Acknowledgment

The first and the last author gratefully acknowledge funding by the DFG GRK 2088.

References

- [AG06] Jean-François Aujol and Guy Gilboa. Constrained and SNR-based solutions for TV-Hilbert space image denoising. *J. Math. Imaging Vision*, 26(1-2):217–237, 2006.
- [AÖ17] Jonas Adler and Ozan Öktem. Solving ill-posed inverse problems using iterative deep neural networks. *Inverse Problems*, 33(12):124007, 2017.
- [AÖ18] Jonas Adler and Ozan Öktem. Learned primal-dual reconstruction. *IEEE transactions on medical imaging*, 37(6):1322–1332, 2018.
- [BBD⁺06] Benjamin Berkels, Martin Burger, Marc Droske, Oliver Nemitz, and Martin Rumpf. Cartoon extraction based on anisotropic image classification vision, modeling, and visualization. In *Vision, Modeling, and Visualization Proceedings*, 2006.
- [BC11] Heinz H. Bauschke and Patrick L. Combettes. *Convex analysis and monotone operator theory in Hilbert spaces*. CMS Books in Mathematics/Ouvrages de Mathématiques de la SMC. Springer, New York, 2011. With a foreword by Hedy Attouch.
- [BLMV10] A. Buades, T.M. Le, J.-M. Morel, and L.A. Vese. Fast cartoon + texture image filters. *IEEE Trans. Image Process.*, 19(8):1978–1986, 2010.

- [BP10] Maïtine Bergounioux and Loic Piffet. A second-order model for image denoising. *Set-Valued Var. Anal.*, 18(3-4):277–306, 2010.
- [BV04] Stephen Boyd and Lieven Vandenberghe. *Convex optimization*. Cambridge University Press, Cambridge, 2004.
- [CCN15] V. Caselles, A. Chambolle, and M. Novaga. Total variation in imaging. In *Handbook of mathematical methods in imaging. Vol. 1, 2, 3*, pages 1455–1499. Springer, New York, 2015.
- [CDOS12] Jian-Feng Cai, Bin Dong, Stanley Osher, and Zuowei Shen. Image restoration: total variation, wavelet frames, and beyond. *J. Amer. Math. Soc.*, 25(4):1033–1089, 2012.
- [Cel69] Arrigo Cellina. Approximation of set valued functions and fixed point theorems. *Ann. Mat. Pura Appl. (4)*, 82:17–24, 1969.
- [CP17] Yunjin Chen and Thomas Pock. Trainable nonlinear reaction diffusion: A flexible framework for fast and effective image restoration. *IEEE transactions on pattern analysis and machine intelligence*, 39(6):1256–1272, 2017.
- [CYP15] Yunjin Chen, Wei Yu, and Thomas Pock. On learning optimized reaction diffusion processes for effective image restoration. In *Proceedings of the IEEE conference on computer vision and pattern recognition*, pages 5261–5269, 2015.
- [EB92] Jonathan Eckstein and Dimitri P. Bertsekas. On the Douglas-Rachford splitting method and the proximal point algorithm for maximal monotone operators. *Math. Programming*, 55(3, Ser. A):293–318, 1992.
- [Gab83] Daniel Gabay. Applications of the method of multipliers to variational inequalities. In *Studies in mathematics and its applications*, volume 15, pages 299–331. Elsevier, 1983.
- [GLMV07] John B. Garnett, Triet M. Le, Yves Meyer, and Luminita A. Vese. Image decompositions using bounded variation and generalized homogeneous Besov spaces. *Appl. Comput. Harmon. Anal.*, 23(1):25–56, 2007.
- [GLT89] Roland Glowinski and Patrick Le Tallec. *Augmented Lagrangian and operator-splitting methods in nonlinear mechanics*, volume 9 of *SIAM Studies in Applied Mathematics*. Society for Industrial and Applied Mathematics (SIAM), Philadelphia, PA, 1989.
- [gra] Test Image Database by the Computer Vision Group of the University of Granada. <http://decsai.ugr.es/cvg/CG/base.htm>. Accessed: 2020-04-30.
- [Jor75] Camille Jordan. Essai sur la géométrie à n dimensions. *Bull. Soc. Math. France*, 3:103–174, 1875.

- [KBPS11] Florian Knoll, Kristian Bredies, Thomas Pock, and Rudolf Stollberger. Second order total generalized variation (tgv) for mri. *Magnetic resonance in medicine*, 65(2):480–491, 2011.
- [LCG18] Yunyi Li, Xiefeng Cheng, and Guan Gui. Co-robust-admm-net: Joint admm framework and dnn for robust sparse composite regularization. *IEEE Access*, 6:47943–47952, 2018.
- [Mal98] S. Mallat. *A wavelet tour of signal processing*. Academic Press, Inc., San Diego, CA, 1998.
- [Mal02] François Malgouyres. Minimizing the total variation under a general convex constraint for image restoration. *IEEE Trans. Image Process.*, 11(12):1450–1456, 2002.
- [Mey01] Y. Meyer. *Oscillating patterns in image processing and nonlinear evolution equations*, volume 22 of *University Lecture Series*. American Mathematical Society, Providence, RI, 2001. The fifteenth Dean Jacqueline B. Lewis memorial lectures.
- [MJU17] Michael T McCann, Kyong Hwan Jin, and Michael Unser. Convolutional neural networks for inverse problems in imaging: A review. *IEEE Signal Processing Magazine*, 34(6):85–95, 2017.
- [MMG12] Anca Morar, Florica Moldoveanu, and Eduard Gröller. Image segmentation based on active contours without edges. In *2012 IEEE 8th International Conference on Intelligent Computer Communication and Processing*, pages 213–220. IEEE, 2012.
- [OR09] Enrique Outerelo and Jesús M. Ruiz. *Mapping degree theory*, volume 108 of *Graduate Studies in Mathematics*. American Mathematical Society, Providence, RI; Real Sociedad Matemática Española, Madrid, 2009.
- [OSV03] Stanley Osher, Andrés Solé, and Luminita Vese. Image decomposition and restoration using total variation minimization and the H^{-1} norm. *Multiscale Model. Simul.*, 1(3):349–370, 2003.
- [Ric19] Robin Richter. *Cartoon-Residual Image Decompositions with Application in Fingerprint Recognition*. PhD thesis, Georg-August-University Göttingen, 2019.
- [ROF92] L.I. Rudin, S. Osher, and E. Fatemi. Nonlinear total variation based noise removal algorithms. *Physica D.*, 60(1-4):259–268, 1992.
- [RTGH] Robin Richter, Hoang-Duy Thai, Carsten Gottschlich, and Stephan Huckemann. Filter design for image decomposition.
- [SB07] Johannes Sveinsson and Jon Benediktsson. Combined wavelet and curvelet denoising of sar images using tv segmentation. In *Geoscience and Remote Sensing Symposium, 2007. IGARSS 2007. IEEE International*, pages 503 – 506, 08 2007.

- [SGG⁺09] Otmar Scherzer, Markus Grasmair, Harald Grossauer, Markus Haltmeier, and Frank Lenzen. *Variational methods in imaging*, volume 167 of *Applied Mathematical Sciences*. Springer, New York, 2009.
- [SWB⁺04] G. Steidl, J. Weickert, T. Brox, P. Mrázek, and M. Welk. On the equivalence of soft wavelet shrinkage, total variation diffusion, total variation regularization, and sides. *SIAM J. Numer. Anal.*, 42(2):686–713, 2004.
- [USVDV09] M. Unser, D. Sage, and D. Van De Ville. Multiresolution monogenic signal analysis using the Riesz-Laplace wavelet transform. *IEEE Trans. Image Process.*, 18(11):2402–2418, 2009.
- [UVDV10] M. Unser and D. Van De Ville. Wavelet steerability and the higher-order Riesz transform. *IEEE Trans. Image Process.*, 19(3):636–652, 2010.
- [VDVBU05] D. Van De Ville, T. Blu, and M. Unser. Isotropic polyharmonic B-splines: scaling functions and wavelets. *IEEE Trans. Image Process.*, 14(11):1798–1813, 2005.
- [VO03] Luminita A. Vese and Stanley J. Osher. Modeling textures with total variation minimization and oscillating patterns in image processing. *J. Sci. Comput.*, 19(1-3):553–572, 2003. Special issue in honor of the sixtieth birthday of Stanley Osher.
- [VO04] Luminita A. Vese and Stanley J. Osher. Image denoising and decomposition with total variation minimization and oscillatory functions. *J. Math. Imaging Vision*, 20(1-2):7–18, 2004. Special issue on mathematics and image analysis.
- [Wan16] Ge Wang. A perspective on deep imaging. *Ieee Access*, 4:8914–8924, 2016.
- [WT10] C. Wu and X.-C. Tai. Augmented Lagrangian method, dual methods, and split Bregman iteration for ROF, vectorial TV, and high order models. *SIAM J. Imaging Sci.*, 3(3):300–339, 2010.
- [YGO05] Wotao Yin, Donald Goldfarb, and Stanley Osher. Image cartoon-texture decomposition and feature selection using the total variation regularized l_1 functional. In *Variational, Geometric, and Level Set Methods in Computer Vision*, pages 73–84. Springer, 2005.
- [YSLX16] Yan Yang, Jian Sun, Huibin Li, and Zongben Xu. Deep admnet for compressive sensing mri. In *30th Conference on Neural Information Processing Systems (NIPS 2016)*, pages 10–18, 2016.

7 Appendix I - Some Basic Mapping Degree Theory

Let $\mathcal{K} \in \mathbb{R}^n$ be the closure of an open bounded set.

Proposition and Definition 7.1 ([OR09], §IV, Prop. and Def. 1.1). Let $g : \mathcal{K} \rightarrow \mathbb{R}^n$ be a differentiable mapping and $p \notin g(\partial\mathcal{K})$ a regular value (with preimage of finite cardinality), then the *degree* $\deg(g, \mathcal{K}, p)$ is defined as:

$$\deg(g, \mathcal{K}, p) := \sum_{x \in g^{-1}(p)} \text{sign}(\det(D_x g)), \quad (7.1)$$

where the sum is 0 in case of $g^{-1}(p) = \emptyset$ and $D_x g$ is the Jacobian matrix at point $x \in \mathcal{K}$.

The notion of degree can be extended to continuous functions.

Proposition and Definition 7.2 ([OR09], §IV, Prop. and Def. 2.1). Let $g : \mathcal{K} \rightarrow \mathbb{R}^n$ be a continuous mapping and $p \notin g(\partial\mathcal{K})$. Then there exists a differentiable mapping $h : \mathcal{K} \rightarrow \mathbb{R}^n$ such that $\|g - h\|_\infty \leq d(p, g(\partial\mathcal{K}))$ and p is a regular value of h . For every such h the *degree* $d(h, \mathcal{K}, p)$ is well-defined and independent of the choice of h , so we can define the degree with respect to g as:

$$\deg(g, \mathcal{K}, p) := \deg(h, \mathcal{K}, p) = \sum_{x \in h^{-1}(p)} \text{sign}(\det(D_x h)).$$

The degree of a continuous function is homotopy-invariant.

Lemma 7.3 ([OR09] §IV, Prop. 2.4). *Let g and h be continuous mappings from \mathcal{K} to \mathbb{R}^n and let $H : [0, 1] \times \mathcal{K} \rightarrow \mathbb{R}^n$ be a homotopy between g and h , i.e. a continuous mapping such that $H(0, \cdot) = g$ and $H(1, \cdot) = h$, such that for all $t \in [0, 1]$ we have $p \notin H(t, \partial\mathcal{K})$, then*

$$\deg(f, \mathcal{K}, p) = \deg(h, \mathcal{K}, p).$$

We will need the following Corollary.

Corollary 7.4 ([OR09], §IV, Cor. 2.5 (2)). *Let $g : \mathcal{K} \rightarrow \mathbb{R}^n$ be a continuous mapping and let $p \notin g(\partial\mathcal{K})$, if $\deg(g, \mathcal{K}, p) \neq 0$ then $p \in \text{Im}(g)$.*

8 Appendix II - Proof of Lemma 4.3

W.l.o.g. assume that Ξ, Ω are linear subspaces, intersecting at the origin $v = 0$, and their sum spans \mathbb{R}^D .

We first show that $\Xi \cap \phi(\Omega) \neq \emptyset$. Suppose that $1 \leq \dim(\Omega) = m < D$, $\dim(\Xi) = D - m$ and choose unit length, pairwise orthogonal vectors $h_1, \dots, h_D \in \mathbb{R}^D$ such that the first m are orthogonal to Ξ and the latter $D - m$ span Ξ . With the matrices $H = (h_1, \dots, h_m)$ and $S = (h_{m+1}, \dots, h_D)$ define the mappings

$$\begin{aligned} \Psi_1 : \Omega &\rightarrow \mathbb{R}^m; \omega \mapsto H^T \omega \\ \Psi_2 : \Omega &\rightarrow \mathbb{R}^m; \omega \mapsto H^T \phi(\omega), \end{aligned} \quad (8.1)$$

and note that $H^T u = 0 \Leftrightarrow u \in \Xi$, as well as

$$\begin{aligned} \|S^T \omega\|^2 &= \sum_{j=m+1}^n (h_j^T \omega)^2 = \max_{\xi \in \Xi, \|\xi\|=1} (\xi^T \omega)^2 \\ &\leq \|\omega\|^2 \max_{\substack{\xi \in \Xi : \|\xi\|=1 \\ \tilde{\omega} \in \Omega : \|\tilde{\omega}\|=1}} (\xi^T \tilde{\omega})^2 = \|\omega\|^2 \cos^2(\theta), \end{aligned}$$

where $\theta \in [0, 1)$ is the first principal angle between Ξ and Ω . Hence, we have for all $\omega \in \Omega$ that

$$\|\Psi_1(\omega)\|^2 = \omega^T (H|S) \begin{pmatrix} H^T \\ S^T \end{pmatrix} \omega - \omega^T S S^T \omega \geq \|\omega\|^2 (1 - \cos^2(\theta)) = \|\omega\|^2 \sin^2(\theta). \quad (8.2)$$

Thus, with the closed ball

$$\mathcal{K} := \left\{ \omega \in \Omega : \|\omega\| \leq C \left(1 + \frac{2}{\sin(\theta)} \right) \right\},$$

in Ω and $\partial\mathcal{K}$, its boundary within Ω , we have in particular for $a \in \partial\mathcal{K}$ that

$$\|\Psi_1(a)\| \geq \|a\| \sin(\theta) = C (\sin(\theta) + 2) \geq 2C. \quad (8.3)$$

Moreover, by hypothesis on ϕ we have for all $a \in \Omega$, in particular for all $a \in \partial\mathcal{K}$, that

$$\|\Psi_2(a) - \Psi_1(a)\| = \|H^T \phi(a) - H^T a\| \leq \|\phi(a) - a\| \leq C, \quad (8.4)$$

by orthonormality of the columns of H .

Now, introducing a homotopy

$$\nu : [0, 1] \times \Omega \rightarrow \mathbb{R}^m, \quad (t, w) \mapsto t\Psi_1(w) + (1-t)\Psi_2(w),$$

between Ψ_1 and Ψ_2 , exploiting (8.3) and (8.4), we have for all $a \in \partial\mathcal{K}$ and $t \in [0, 1]$ that

$$\begin{aligned} \|\nu(t, a)\| &= \|t\Psi_1(a) + (1-t)\Psi_2(a)\| \\ &= \|\Psi_1(a) - (1-t)(\Psi_1(a) - \Psi_2(a))\| \\ &\geq \|\Psi_1(a)\| - \|(1-t)(\Psi_1(a) - \Psi_2(a))\| \geq C, \end{aligned}$$

yielding

$$\nexists (t, a) \in [0, 1] \times \partial\mathcal{K} \text{ such that } \nu(t, a) = 0. \quad (8.5)$$

Finally, let $B = (b_1, \dots, b_m)$ with an orthonormal basis b_1, b_2, \dots, b_m of Ω and define the isomorphism

$$f : \mathbb{R}^m \rightarrow \Omega, \quad x \mapsto Bx.$$

Then

$$\nu_f : [0, 1] \times f^{-1}(\mathcal{K}), \quad (t, x) \mapsto \nu(t, f(x)),$$

is a homotopy between the isomorphism $\Psi_1 \circ f : \mathbb{R}^m \rightarrow \mathbb{R}^m$ and $\Psi_2 \circ f$, and by (8.5) we have

$$\nexists (t, a) \in [0, 1] \times (f^{-1}(\partial\mathcal{K})) \text{ such that } \nu_f(t, a) = 0.$$

Hence, we can apply Lemma 7.3 to obtain

$$\begin{aligned}
\deg(\Psi_2 \circ f, f^{-1}(\mathcal{K}), 0) &= \deg(\Psi_1 \circ f, f^{-1}(\mathcal{K}), 0) \\
&= \text{sign}(\det(D_0[\Psi_1 \circ f])) \\
&= \text{sign}(\det(D_0[\Psi_1]D_0[f])) \\
&= \text{sign}(\det(H^T B)) \neq 0.
\end{aligned}$$

By Corollary 7.4 we obtain the existence of at least one $x \in \mathbb{R}^m$ such that $H^T(\phi \circ f)(x) = 0$, yielding that there must exist at least one $\omega \in \phi(\Omega)$ such that $H^T\omega = 0$. By construction of H such an ω is in Ξ proving the first assertion.

Next, we show the asserted inequality. Let $u = \phi(\omega) \in \Xi \cap \phi(\Omega)$ with $\omega \in \Omega$. Then, we have $\|u - \omega\| \leq C$ by hypothesis on ϕ and by (8.4) that

$$\|\Psi_1(\omega)\| = \|H^T\omega\| = \|H^T\omega - H^T u\| = \|\Psi_1(\omega) - \Psi_2(\omega)\| \leq C.$$

Furthermore, by (8.2) we have

$$\|\omega\| \leq \frac{C}{\sin(\theta)},$$

yielding finally,

$$\|u\| \leq \|u - \omega\| + \|\omega\| \leq C \left(1 + \frac{1}{\sin(\theta)}\right).$$

9 Appendix III - Detail to Separating Cartoon and Texture

Recalling (5.2) and (5.3) introduce the *refinement filter function*

$$h_\gamma(x, y) := \frac{2\widehat{f}_\gamma(-2x, -2y)}{\widehat{f}_\gamma(-x, -y)},$$

see [VDVBU05, Eq.(29)], obtain for a scale $j \in \{0, 1, \dots, J-1, J\}$ via dyadic subsampling (cf. [Mal98]) the primal wavelet frames $T_{j,s}^{\text{primal}} \in \mathbb{R}^{n \times m}$, for $s = 1, 2, 3$,

$$\begin{aligned}
T_{j,1}^{\text{primal}}[k, \ell] &= \frac{1}{2} \exp(-i(2^{j-1}\omega_k + \pi)) h_\gamma(2^{j-1}\omega_k + \pi, 2^{j-1}\omega_\ell) \\
&\quad \times a_\gamma(2^{j-1}\omega_k + \pi, 2^{j-1}\omega_\ell) \widehat{f}_\gamma(2^{j-1}\omega_k, 2^{j-1}\omega_\ell), \\
T_{j,2}^{\text{primal}}[k, \ell] &= \frac{1}{2} \exp(-i(2^{j-1}\omega_k + \pi)) h_\gamma(2^{j-1}\omega_k, 2^{j-1}\omega_\ell + \pi) \\
&\quad \times a_\gamma(2^{j-1}\omega_k, 2^{j-1}\omega_\ell + \pi) \widehat{f}_\gamma(2^{j-1}\omega_k, 2^{j-1}\omega_\ell), \\
T_{j,3}^{\text{primal}}[k, \ell] &= \frac{1}{2} \exp(-i(2^{j-1}\omega_k + \pi)) h_\gamma(2^{j-1}\omega_k + \pi, 2^{j-1}\omega_\ell + \pi) \\
&\quad \times a_\gamma(2^{j-1}\omega_k + \pi, 2^{j-1}\omega_\ell + \pi) \widehat{f}_\gamma(2^{j-1}\omega_k, 2^{j-1}\omega_\ell).
\end{aligned} \tag{9.1}$$

and their dual counterparts

$$\begin{aligned}
T_{j,1}^{\text{dual}}[k, \ell] &= \frac{1}{2} \exp(-i(2^{j-1}\omega_k + \pi)) \frac{h_\gamma(2^{j-1}\omega_k + \pi, 2^{j-1}\omega_\ell)}{a_\gamma(2^j\omega_k, 2^j\omega_\ell)} \\
&\quad \times \frac{\widehat{f}_\gamma(2^{j-1}\omega_k, 2^{j-1}\omega_\ell)}{a_\gamma(2^{j-1}\omega_k, 2^{j-1}\omega_\ell)}, \\
T_{j,2}^{\text{dual}}[k, \ell] &= \frac{1}{2} \exp(-i(2^{j-1}\omega_k + \pi)) \frac{h_\gamma(2^{j-1}\omega_k, 2^{j-1}\omega_\ell + \pi)}{a_\gamma(2^j\omega_k, 2^j\omega_\ell)} \\
&\quad \times \frac{\widehat{f}_\gamma(2^{j-1}\omega_k, 2^{j-1}\omega_\ell)}{a_\gamma(2^{j-1}\omega_k, 2^{j-1}\omega_\ell)}, \\
T_{j,3}^{\text{dual}}[k, \ell] &= \frac{1}{2} \exp(-i(2^{j-1}\omega_k + \pi)) \frac{h_\gamma(2^{j-1}\omega_k + \pi, 2^{j-1}\omega_\ell + \pi)}{a_\gamma(2^j\omega_k, 2^j\omega_\ell)} \\
&\quad \times \frac{\widehat{f}_\gamma(2^{j-1}\omega_k, 2^{j-1}\omega_\ell)}{a_\gamma(2^{j-1}\omega_k, 2^{j-1}\omega_\ell)}.
\end{aligned} \tag{9.2}$$

Further we link the isotropic polyharmonic B-splines to the Z -th order *Riesz transform* in order to model directionality, cf. [USVDV09] and [UVDV10, Eqns. (4) and (10)], and define for $z = 1, 2, \dots, Z$ the matrices $R_z \in \mathbb{R}^{n \times m}$ by

$$R_z[k, \ell] := (-i)^Z \sqrt{\frac{Z!}{z!(Z-z)!}} \frac{\omega_k^z \omega_\ell^{Z-z}}{(\omega_k^2 + \omega_\ell^2)^{\frac{Z}{2}}}.$$

Now we are ready to define \underline{B} and $\widetilde{\underline{B}}$. For $j = 0, \dots, J$, $z = 1, \dots, Z$, $s = 1, 2, 3$ define

$$\begin{aligned}
\widehat{B}_{j,z,s}[k, \ell] &= T_{j,s}^{\text{primal}}[k, \ell] R_z[k, \ell] \\
\widetilde{\widehat{B}}_{j,z,s}[k, \ell] &= T_{j,s}^{\text{dual}}[k, \ell] R_z[k, \ell].
\end{aligned}$$

From (9.1) and (9.2) we have at once the factor matrix-family of $(\underline{B}, \widetilde{\underline{B}})$

$$\begin{aligned}
\widehat{Y}_{j,z,1}[k, \ell] &= (a_\gamma(2^{j-1}\omega_k + \pi, 2^{j-1}\omega_\ell) a_\gamma(2^{j-1}\omega_k, 2^{j-1}\omega_\ell) a_\gamma(2^j\omega_k, 2^j\omega_\ell))^{-1}, \\
\widehat{Y}_{j,z,2}[k, \ell] &= (a_\gamma(2^{j-1}\omega_k, 2^{j-1}\omega_\ell + \pi) a_\gamma(2^{j-1}\omega_k, 2^{j-1}\omega_\ell) a_\gamma(2^j\omega_k, 2^j\omega_\ell))^{-1}, \\
\widehat{Y}_{j,z,3}[k, \ell] &= (a_\gamma(2^{j-1}\omega_k + \pi, 2^{j-1}\omega_\ell + \pi) a_\gamma(2^{j-1}\omega_k, 2^{j-1}\omega_\ell) a_\gamma(2^j\omega_k, 2^j\omega_\ell))^{-1}.
\end{aligned}$$

Since $\widehat{Y}_{j_1, z_1, s_1} \neq \widehat{Y}_{j_2, z_2, s_2}$ for $j_1 \neq j_2$ or $s_1 \neq s_2$ we have that $(\underline{B}, \widetilde{\underline{B}})$ is weakly but not strongly factoring.

In the numerical implementation, we approximate the infinite sum in (5.4) by

$$a_\gamma(x, y) := \sum_{r,s \in \{-10, \dots, 10\}} \left(\widehat{f}_\gamma(x + 2\pi r, y + 2\pi s) \right)^2.$$

Further due to correction by H in equation (5.5), the resulting entries of the filters $\underline{B}^{\text{cor}}$ and $\widetilde{\underline{B}}^{\text{cor}}$, when transformed back to the spacial domain, have small, but non-zero imaginary parts. We cut these imaginary parts off. Since we defined filters with real entries in the frequency domain, by removing their imaginary part in the spatial domain, the matrix entries in the frequency domain remain real, so that all eigenvalues of the thus adjusted $\underline{\mathfrak{C}}_{\widetilde{\underline{B}}}^* \underline{\mathfrak{C}}_{\underline{B}}$ are real and the factor

matrix-family has real entries, making the resulting filters weakly factoring. Since we have

$$\begin{aligned}
& \left| \sum_{j,n,s} \overline{\widehat{B}_{j,n,s}^{\text{cor}}[k,\ell]} \widehat{B}_{j,n,s}^{\text{cor}}[k,\ell] \right| \\
&= \left| \left(\sum_{j,n,s} \overline{\widetilde{B}_{j,n,s}[k,\ell]} \widehat{B}_{j,n,s}[k,\ell] \right) \left(\widehat{A}[k,\ell] + \sum_{j,n,s} \overline{\widetilde{B}_{j,n,s}[k,\ell]} \widehat{B}_{j,n,s}[k,\ell] \right)^{-1} \right| \\
&\leq 1
\end{aligned}$$

and observe that the above sum on the left-hand-side only gets smaller if the imaginary parts of \underline{B} , \widetilde{B} are removed, the resulting filters satisfy the (NEPC). In all experiments conducted in this paper numerically the above inequality was strict, so that all filters used for the LbS model satisfied the (CPC).

10 Appendix IV - More Cartoons

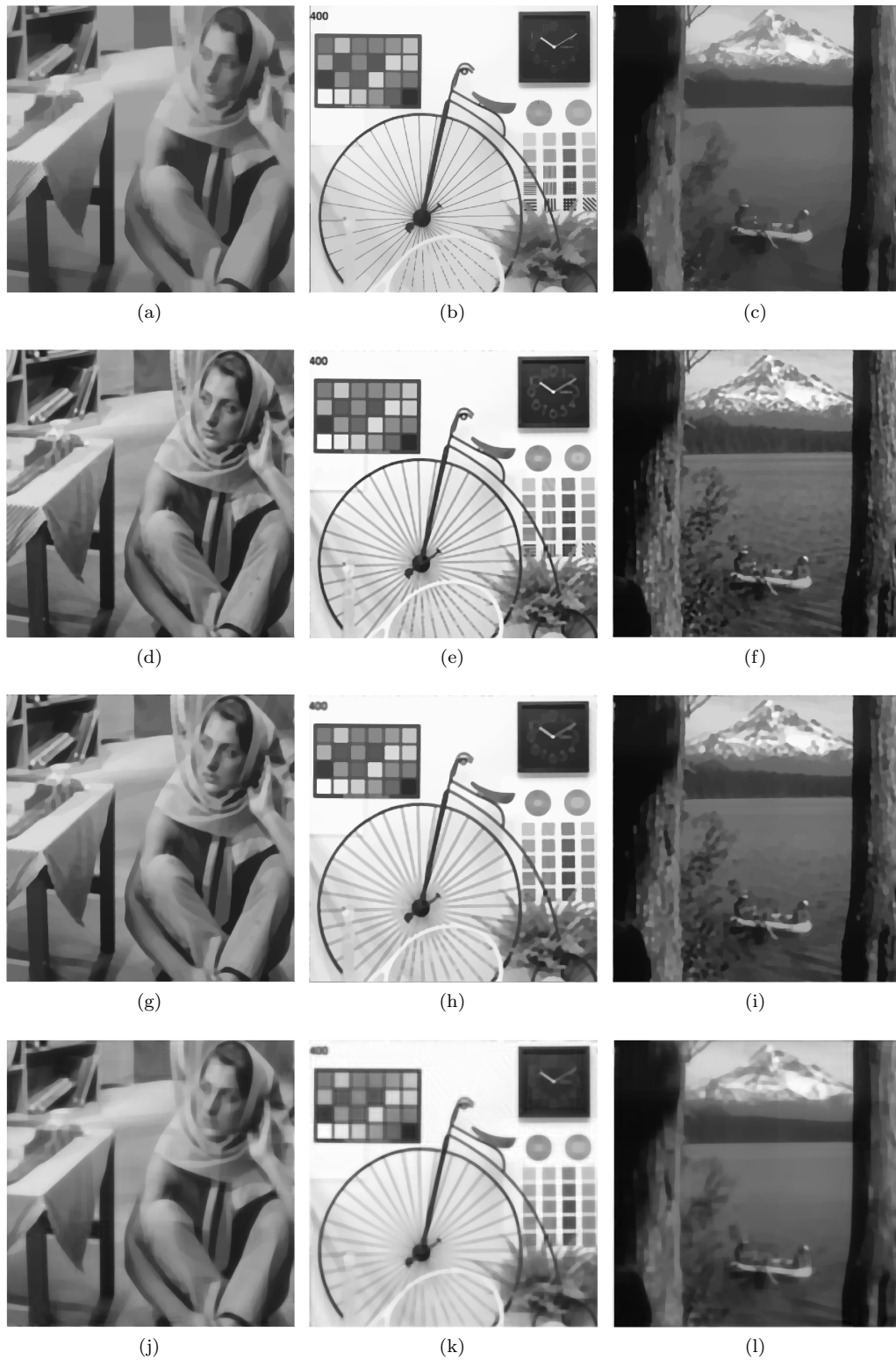


Figure 3: Cartoons computed from the test images barbara, bicycle, lake from Figure 1 (see [gra] and) via $TV - \ell^2$ (1st row: a-c), OSV (2nd row: d-f), TV -Hilbert (3rd row: g-i) and the proposed LsR (4th row: j-l).

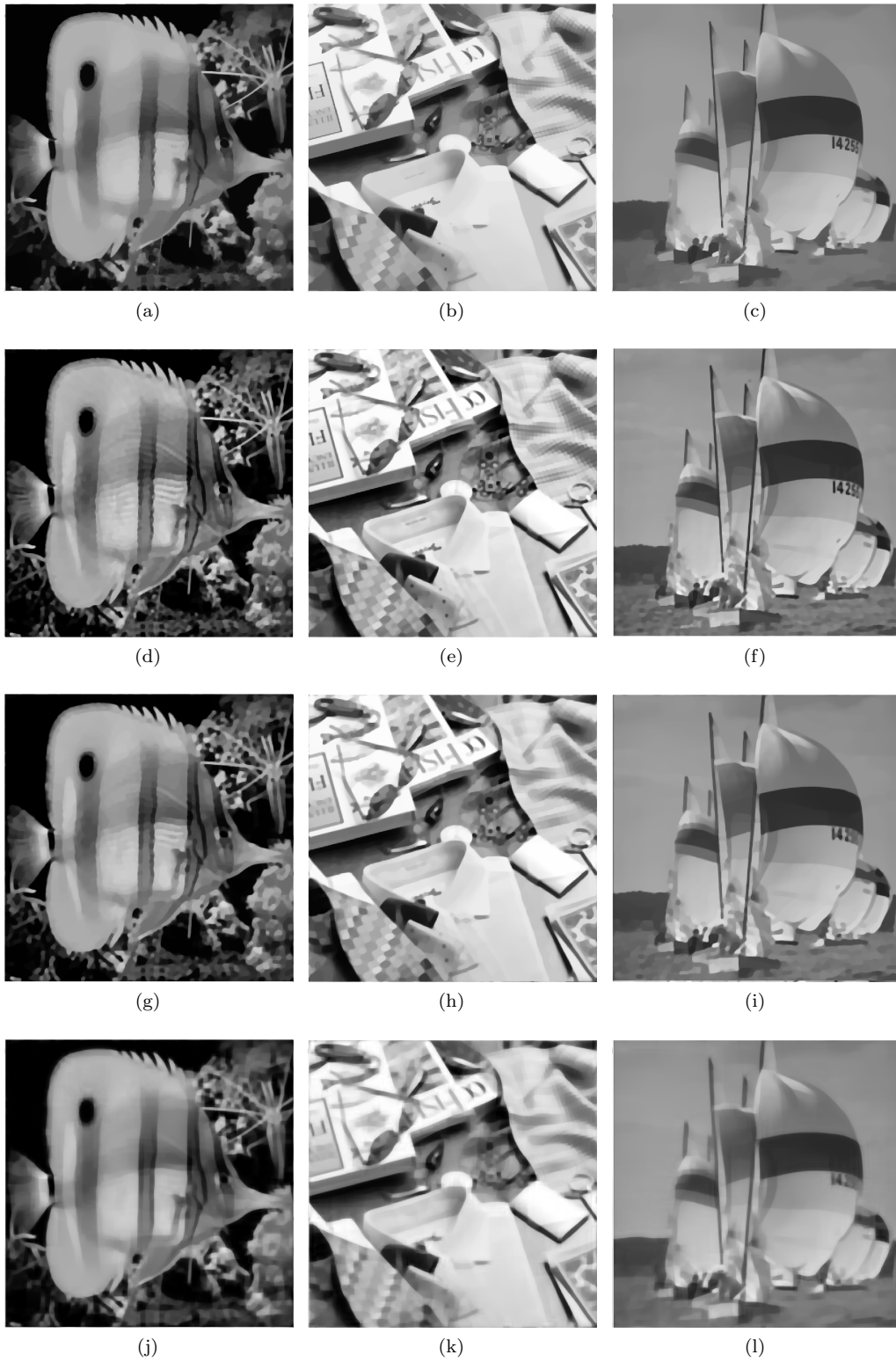


Figure 4: Cartoons computed from the test fish, clutter, sail from Figure 2 (see [gra] and) via $TV - \ell^2$ (1st row: a-c), OSV (2nd row: d-f), TV -Hilbert (3rd row: g-i) and the proposed LsR (4th row: j-l).